

Constructing an entangled Unruh Otto engine and its efficiency

Dipankar Barman*, Bibhas Ranjan Majhi†

Department of Physics, Indian Institute of Technology Guwahati,
Guwahati 781039, Assam, India

April 19, 2022

Abstract

Uniformly accelerated frame mimics a thermal bath whose temperature is proportional to the proper acceleration. Using this phenomenon we give a detailed construction of an Otto cycle between two energy eigenstates of a system, consists of two entangled qubits. In the isochoric stages the thermal bath is being provided via the vacuum fluctuations of the background field for a monopole interaction by accelerating them. We find that making of Otto cycle is possible when one qubit is accelerating in the right Rindler wedge and other one is moving in the left Rindler wedge; i.e. in anti-parallel motion, with the initial composite state is a non-maximally entangled one. However, the efficiency greater than that of the usual single qubit quantum Otto engine is not possible. We provide values of the available parameters which make Otto cycle possible. On the other hand, Otto cycle is not possible if one considers the non-maximally entangled state for parallel motion. Moreover, for both initial symmetric and anti-symmetric Bell states we do not find any possibility of the cycle for qubits' parallel and anti-parallel motion.

1 Introduction

Thermodynamics of a quantum system has been a very active area and considerable amount of effort has been devoted to develop a fruitful theoretical formalism in order to explore the quantum thermodynamics. The definition of work, energy and heat of a quantum system is properly addressed in this paradigm. Consider a quantum system, described by a density operator $\rho(t)$, is evolving under a time dependent Hamiltonian $H_0(t)$. The variation of the expectation value of the energy, $\Delta\langle E \rangle$ from time t_i to t_f satisfies [1]

$$\Delta\langle E \rangle = \langle Q \rangle + \langle W \rangle, \quad (1)$$

where we identify

$$\Delta\langle E \rangle = \int_{t_i}^{t_f} dt \frac{d}{dt} \langle E \rangle; \quad (2)$$

$$\langle Q \rangle = \int_{t_i}^{t_f} dt \text{Tr} \left(\frac{d\rho(t)}{dt} H_0 \right); \quad (3)$$

and

$$\langle W \rangle = \int_{t_i}^{t_f} dt \text{Tr} \left(\rho(t) \frac{dH_0}{dt} \right), \quad (4)$$

as total energy change, heat transfer and work done on the system, respectively. The above concepts of different thermodynamic quantities has been successfully implemented to construct quantum version of different classical engines; e.g. Carnot engine, Otto engine, *etc.* [2, 3, 4, 5, 6]. A Quantum Otto Engine

*E-mail: dipankar1998@iitg.ac.in

†E-mail: bibhas.majhi@iitg.ac.in

(QOE) can be constructed with a single qubit [3, 4], which has four steps. The system undergoes two adiabatic processes and two isochoric processes. In adiabatic process, there is work done on or by the system and in isochoric process, system has heat exchange with the environment. The efficiency turns out to be

$$\eta_0 = 1 - \frac{\omega_1}{\omega_2}, \quad (5)$$

with $\eta_0 < 1$. Here ω_1 (ω_2) is the energy gap before (after) the adiabatic expansion of the levels of the qubit. Note that, contrary to the classical Otto engine in which efficiency depends on the temperatures of the thermal baths during the isochoric processes, η_0 for QOE depends on the energy gaps between the quantum levels of the qubit system.

On the other hand the combination of relativity and quantum mechanics, best described by quantum field theory, brings several interesting and important phenomenon, like Hawking [7, 8] and Unruh [9, 10, 11] effects, in front of us. These two phenomenon naturally create a thermal environment for a specific class of observers. Recently, using the concept of Unruh phenomenon [9, 10, 11], a Unruh quantum Otto engine (UQOE) has been proposed in [12, 13, 14]. This, contrary to QOE, is a completely relativistic set up and therefore the measured time in each stages is denoted by qubit's proper time (so the role of time parameters t in Eqs. (2) – (4) is played by proper time τ of qubit's frame). According to the Unruh effect, a uniformly accelerating observer can see particles in the Minkowski vacuum and this acts as the thermal bath for the accelerating frame. The temperature of the bath which is proportional to the proper acceleration can be utilised as heat source for an Otto cycle. So the hot (cold) thermal baths during the isochoric processes can be mimicked by giving uniformly acceleration (deceleration) to the qubit. This is known as Unruh Quantum Otto Engine (UQOE). The efficiency of this cycle came out to be that given in (5) (see [12, 13], for details).

Using the idea of UQOE, one of the authors of this paper with Kane very recently proposed a quantum Otto cycle consists of two entangled qubits [15]. The underlying inspiration comes from the fact that Unruh effect is greatly influenced by entanglement between the accelerated observer with another accelerated frame [16, 17, 18, 19]. Moreover the entanglement phenomenon itself is observer dependent quantity [20, 21, 22, 23]. In this regard it may also be noted that the quantum entanglement harvesting between two causally disconnected accelerated detectors is possible within a relativistic setup. All these events imply a possibility of considerable influence on the efficiency of engines when one considers the cycle between entangled states of two accelerated qubits. The analysis in [15] revealed that the efficiency for the cycle between an entangled state and their collective excited state, depending on the relative accelerations of the qubits during the isochoric process, may vary from a standard quantum Otto cycle. This is named as Entangled Unruh Quantum Otto Engine (EUQOE).

In this paper we will readdress this EUQOE and its nature of efficiency in a much more broader perspective. Moreover the analysis in [15] is found to have few limitations and is not complete. Let us now mention them.

- To make a cycle efficient for work output, the amount of work done has to be positive. In addition during the isochoric processes the heat absorption (rejection) must happen in order to make a fruitful engine. We will see later that these are supplemented by condition given by Eq. (11) (see also below Eq. (25) of [15]). In order to fulfilment of these one must choose the values of the available parameters (e.g. accelerations of the qubits, the spacing of energy levels of the qubits, the interaction time during isochoric phases, *etc.*), appearing in the system. This identification of the parameter space of all these quantities has not been done earlier. Therefore it is not clear whether any such parameter space is available in all practical purposes in order to construct a EUQOE.
- The time evolution of the state of system has been done by assuming the satisfaction of commutation between different time Hamiltonians. But we know that in general this may not be always true and in that situation time-ordering is necessary.
- In the existing analysis considered that the two qubits are accelerating in the same side of the Rindler wedge (right Rindler wedge (RRW)) during the isochoric stages. But we know that accelerated frame can be constructed in the left Rindler wedge (LRW) as well. Also since the frames, accelerating in these two opposite wedges, can harvest quantum entanglement [24, 25], it would be interesting to incorporate this situation in constructing EUQOE. Such generalization was absent in [15]. Therefore, the question of the possibility of making a EUQOE when one detector is accelerating in the right and another in the left Rindler wedge remains an option to investigate.

Here we aim to present a complete picture of the EUQOE. All the gaps, mentioned above, will be addressed here. We scan the parameter space for which making of a EUQOE is possible. Here for simplicity, we always fix the ratio of the acceleration of the detectors. We observed that the necessary conditions are not getting satisfied when both detectors are in the right Rindler wedge with any initially entangled state of the detectors. We also observe that either maximally symmetric or anti-symmetric both do not lead to any fruitful cycle when the qubits are accelerating in two opposite Rindler wedges. The construction of Otto engine is prohibited by the dissatisfaction of the required conditions. However, making of EUQOE is possible with initially non-maximally entangled states for detectors are in anti-parallel motion. However, the efficiency get suppressed for all the parameter values. The efficiency of the cycle depends on the acceleration of the first detector, ratio of the detectors A 's acceleration to detector B 's acceleration and the energy gap of the composite system. Therefore we can regulate the efficiency of the cycle by tuning these parameters.

The organization of the paper is as follows. In Section 2 we begin with a brief description on our model. This section also describes the stages of our EUQOE and provides the expression of the efficiency of the cycle in terms of elements of time evolved density matrix of the two detectors' system. In the next Section 3 we provide the expressions of elements of the density matrix for the detectors are accelerating in same and opposite Rindler wedges. Thereafter, we analyzed for the possibility of making an EUQOE in various possible parameter spaces. Finally, we conclude this article in Section 4 with discussion of our results. Five appendices are also provided at the end in order to show the explicit steps to evaluate several important relations and results.

2 Set Up

We construct a similar system as considered in [15]. It consists of two identical qubits (chosen as two level Unruh De-Witt detectors [26]), A and B , having energy levels with energy $g_j = -\omega/2$ for the ground state and $e_j = \omega/2$ for the excited state. The corresponding eigenkets are $|g_j\rangle$ and $|e_j\rangle$ (where $j = A, B$), respectively. The free Hamiltonian of the detectors can be chosen as [16, 27]

$$H_0 = \frac{\omega(\tau)}{2} \left(\frac{d\tau_A}{d\tau} S_A^z \otimes \mathbf{1}_B + \frac{d\tau_B}{d\tau} \mathbf{1}_A \otimes S_B^z \right), \quad (6)$$

where $S_j^z = (|e_j\rangle\langle e_j| - |g_j\rangle\langle g_j|)$, ω is the energy gap of the detectors and τ_A, τ_B are the proper times of the respective detectors. In the above τ is the proper time of our observer which we choose as the detector A and hence $\tau = \tau_A$. Same Hamiltonian has been chosen earlier in various investigations [16, 27]. The energy eigenstates and the corresponding eigenvalues can be obtained for the composite system as

$$\begin{aligned} E_e = \omega, \quad |e\rangle &= |e_A\rangle|e_B\rangle; \\ E_s = 0, \quad |s\rangle &= \frac{1}{\sqrt{2}}(|e_A\rangle|g_B\rangle + |g_A\rangle|e_B\rangle); \\ E_a = 0, \quad |a\rangle &= \frac{1}{\sqrt{2}}(|e_A\rangle|g_B\rangle - |g_A\rangle|e_B\rangle); \\ E_g = -\omega, \quad |g\rangle &= |g_A\rangle|g_B\rangle; \end{aligned} \quad (7)$$

Here, as discussed in [15, 19] transition from $|g\rangle \rightarrow |e\rangle$ or $|e\rangle \rightarrow |g\rangle$ is not possible for the following type of interaction between the background real scalar field and monopole detectors [28, 29, 24, 19, 25]:

$$H_{int} = \sum_{j=A,B} c_j \chi_j(\tau) m_j(\tau_j) \phi(x_j(\tau_j)) \frac{d\tau_j}{d\tau}. \quad (8)$$

In the above c_j is coupling constant of interaction. We choose $c_A = c_B = c$, as the detectors in our case are identical. For our present purpose we will use this type of interaction. The monopole operator of j -th detector, m_j at the initial time is defined by

$$m_j(0) = |e_j\rangle\langle g_j| + |g_j\rangle\langle e_j|. \quad (9)$$

It has been shown in [19] that the transition probability from $|a\rangle \rightarrow |e\rangle$ and $|a\rangle \rightarrow |g\rangle$ are same, as they have same energy spacing. Similarly the probabilities for the transitions $|s\rangle \rightarrow |e\rangle$ and $|s\rangle \rightarrow |g\rangle$ are also

same. Notice that $|s\rangle$ and $|a\rangle$ are two Bell states appearing in the composite system which are maximally entangled ones. Moreover, for a general initial state, $|D\rangle = b_1|e_Ag_B\rangle + b_2|g_Ae_B\rangle$ with $E_D = 0$, transition probabilities $|D\rangle \rightarrow |e\rangle$ and $|D\rangle \rightarrow |g\rangle$ are also same. With the above information here we can try to construct the Otto cycle between $|s\rangle$ and $|e\rangle$ or $|g\rangle$, $|a\rangle$ and $|e\rangle$ or $|g\rangle$ (also between $|D\rangle$ and $|e\rangle$ or $|g\rangle$), for maximally and non-maximally (depending on the values of b_1 and b_2 with $b_1^2 + b_2^2 = 1$) entangled states. We will check all of these possibilities here.

We choose the detector A as our primary observer. Therefore we set $\tau = \tau_A$ and define $d\tau_B/d\tau = \alpha$ which is constant during detectors' motions with uniform velocities as well as uniform accelerations (see [17] for relation between τ_A and τ_B ; an additional discussion has been given in Appendix A as well). Later for notational convenience, we will add a subscript with α : v for constant velocity and a_k ($k = H, C$) for uniform acceleration in heating process (H) and cooling process (C). We have calculated α 's for different stages of the cycle in Appendix A. The free Hamiltonian (6) can be represented as

$$H_0 = \frac{\omega}{2} \begin{pmatrix} (1 + \alpha) & 0 & 0 & 0 \\ 0 & (1 - \alpha) & 0 & 0 \\ 0 & 0 & (-1 + \alpha) & 0 \\ 0 & 0 & 0 & (-1 - \alpha) \end{pmatrix} = \omega h_\alpha, \quad (10)$$

in the basis $\{|e_Ae_B\rangle, |e_Ag_B\rangle, |g_Ae_B\rangle, |g_Ag_B\rangle\}$.

2.1 Stages of cycle

The stages of our EUQOE are already being discussed in [15] which are along the line of those given in [12, 13] for UQOE. For convenience, here again let us briefly describe the stages of the cycle.

- *Adiabatic expansion:* In step I, the detectors A and B travel at velocities $-v_A$ and $-v_B$ (v_B for anti-parallel motion) for time intervals $\Delta\tau_A^1$ and $\Delta\tau_B^1$, respectively (here superscripts for the stage number and subscripts for detectors). In this process work is done on the composite system, so that the energy gap increased from the initial gap ω_1 to ω_2 . However, the population density of the states remain unchanged.
- *Heat absorption through isochoric process:* After step I, the detectors started accelerating with proper accelerations a_{A_H} and a_{B_H} , respectively. Due to acceleration, the detectors perceives the Minkowski vacuum as thermal bath as a result of interaction between the detectors and the background quantum fields. The system then absorbs the heat. The detectors accelerate for the time intervals $\Delta\tau_A^2$ and $\Delta\tau_B^2$, when their velocities changes from $-v_A$ to v_A and $-v_B$ to v_B (or v_B to $-v_B$), respectively. As the density matrix evolve under the interaction, it goes from initial state ρ_0 to $\rho_0 + \delta\rho^H$. The expressions of $\delta\rho^H$ for general $\rho_0 = |D\rangle\langle D|$ is explicitly calculated in Appendix B (see final expression in (B.26)).
- *Adiabatic Compression:* The interaction with the background field in this stage is turned off and the population density of the states remain unchanged. The detectors started moving with constant velocity, v_A and v_B (or $-v_B$) for the time intervals of $\Delta\tau_A^3$ and $\Delta\tau_B^3$, respectively. The energy spacing of the system is allowed to decrease from ω_2 to ω_1 .
- *Heat ejection through isochoric process:* In the final stage, the detectors started decelerating with proper uniform decelerations a_{A_C} and a_{B_C} , respectively. As a result, their velocities changes from v_A to $-v_A$ and v_B to $-v_B$ (or $-v_B$ to v_B), respectively. The temperature of background quantum vacuum is taken to be lower by considering $a_{j_C} < a_{j_H}$. This can be done by taking longer interaction time intervals $\Delta\tau_A^4$ and $\Delta\tau_B^4$ compared to those in stage II. Then the system transfers heat to the environment. The density of state goes from $\rho_0 + \delta\rho^H$ to $\rho_0 + \delta\rho^H + \delta\rho^C$. To maintain the cyclicity of the engine, we impose a constraint, $\delta\rho^H + \delta\rho^C = 0$.

2.2 Efficiency

For the cycle to be efficient to work, one has to insure the positivity of work done and heat absorption by the engine. This is being confirmed by the following impositions [15]:

$$\text{Tr}(\delta\rho^H h_{\alpha_k}) > 0; \quad (k = v, a_H, a_C). \quad (11)$$

This condition must be satisfied by the EUQOE. The conservation of energy requires [15]

$$\omega_2 \text{Tr}(\delta\rho^H h_{\alpha_{a_H}}) - \omega_1 \text{Tr}(\delta\rho^H h_{\alpha_{a_C}}) = (\omega_2 - \omega_1) \text{Tr}(\delta\rho^H h_{\alpha_v}). \quad (12)$$

The efficiency of our EUQOE can be obtained as [15]

$$\eta_E = \left(1 - \frac{\omega_1}{\omega_2}\right) \frac{\text{Tr}(\delta\rho^H h_{\alpha_v})}{\text{Tr}(\delta\rho^H h_{\alpha_{a_H}})} = \eta_0 \frac{\text{Tr}(\delta\rho^H h_{\alpha_v})}{\text{Tr}(\delta\rho^H h_{\alpha_{a_H}})}. \quad (13)$$

Simultaneous satisfaction of the conditions (11), (12) and (13) guarantees that $\eta_E < 1$ (see [15] for all these details). Note that the factor, appearing on the right hand side with η_0 , contains the variation of the density matrix ($\delta\rho^H$) only for the second stage, i.e. in the isochoric heating process. This factor is always greater than zero due to the positivity of the work done, heat absorption and heat rejection by the engine, and so $(\eta_E/\eta_0) > 0$. Now in order to make EUQOE more efficient than the UQOE we must have $(\eta_E/\eta_0) > 1$; i.e. $\frac{\text{Tr}(\delta\rho^H h_{\alpha_v})}{\text{Tr}(\delta\rho^H h_{\alpha_{a_H}})} > 1$, under the constraint $\eta_0 < 1$ and $\eta_E < 1$. In this case, the efficiency (η_E) of the engine will be increased due to entanglement phenomenon. However, the efficiency (η_E) will always be less than one. We mention that the expression for efficiency (13) reduced to a very simple form in [15] for the initial state as $|a\rangle$ and $|s\rangle$. We found that such is due to the calculation of traces in (13) without proper time ordering in the perturbative expansion. Here we will improve this analysis by incorporating the time ordering prescription.

The explicit expressions of the trace quantities in (13), incorporating the time ordering, have been calculated in Appendix C through perturbation technique, described in Appendix B. The first relevant contribution is coming in the second order. Considering till this order we obtain $\text{Tr}(\delta\rho^H h_\alpha)$ as (see Eq. (C.5))

$$\text{Tr}(\delta\rho^H h_\alpha) = \{b_2^2 \mathcal{P}_A(\omega) - b_1^2 \mathcal{P}_A(-\omega)\} + b_1 b_2 \Delta \mathcal{P}_{AB} + \alpha \{ (b_1^2 \mathcal{P}_B(\omega) - b_2^2 \mathcal{P}_B(-\omega)) + b_1 b_2 \Delta \mathcal{P}_{AB} \}. \quad (14)$$

The expressions of the relevant quantities are given by

$$\mathcal{P}_j(\omega_2) = c^2 \int \int d\tau_j d\tau'_j \chi_j(\tau_j) \chi_j(\tau'_j) G^+(\bar{x}'_j, \bar{x}_j) e^{i\omega_2(\tau_j - \tau'_j)}; \quad (j = A, B), \quad (15)$$

and

$$\Delta \mathcal{P}_{AB} = \mathcal{P}_{AB}(\omega_2, -\omega_2) - \mathcal{P}_{AB}(-\omega_2, \omega_2), \quad (16)$$

where

$$\mathcal{P}_{AB}(\omega_2, -\omega_2) = c^2 \int \int d\tau_A d\tau'_B \chi_A(\tau_A) \chi_B(\tau'_B) e^{i\omega_2(\tau_A - \tau'_B)} G^+(\bar{x}'_B, \bar{x}_A), \quad (17)$$

with $\mathcal{P}_j(-\omega_2)$ and $\mathcal{P}_{AB}(-\omega_2, \omega_2)$ are obtained by replacing $\omega_2 \rightarrow -\omega_2$ in the *integrands* of (15) and (17). For maximally entangled initial states, $b_1 = \pm b_2 = 1/\sqrt{2}$, (14) get further simplified by introducing $\Delta \mathcal{P}_j = \mathcal{P}_j(\omega) - \mathcal{P}_j(-\omega)$. In the above quantities, $G^+(\bar{x}'_j, \bar{x}_j)$ is the positive frequency Wightman function. These integrations are calculated during the stage II of the cycle, where ω_2 is energy gap of the engine. We do not need to evaluate the same for stage IV of the cycle due to the cyclicity condition.

3 Calculation of efficiency

In order to find the explicit value of η_E in Eq. (13) one needs to evaluate the integrations (15) and (17). Note that in the second stage, the interaction time is $\Delta\tau_j^2$ for the j -th detector ($j = A, B$). This time is the time required for changing the velocity from $-v_j$ to v_j and can be determined in the following way.

For RRW, the relations between the Rindler proper time and the Minkowski coordinates are

$$t_j = \frac{1}{a_{j_k}} \sinh(a_{j_k} \tau_j); \quad x_j = \frac{1}{a_{j_k}} \cosh(a_{j_k} \tau_j), \quad (18)$$

where index k can be H (C) denoting heating process (cooling process). Now velocity is given by $v_j = (dx_j/dt_j) = (dx_j/d\tau_j)/(dt_j/d\tau_j) = \tanh(a_{j_k} \tau_j)$ and this determines the time interval as $(2/a_{j_k}) \tanh^{-1}(v_j)$ when the detector is accelerating on the RRW. Here we define $\mathcal{T}_{j_k}/2 = (1/a_{j_k}) \tanh^{-1}(v_j)$ for that, and then the integration limits will be from $-\mathcal{T}_{j_k}/2$ to $\mathcal{T}_{j_k}/2$.

On the other hand, if the detector is accelerating in the LRW, then the coordinate relations are

$$t_j = \frac{1}{a_{j_k}} \sinh(a_{j_k} \tau_j); \quad x_j = -\frac{1}{a_{j_k}} \cosh(a_{j_k} \tau_j). \quad (19)$$

Now the velocities are given by $v_j = -\tanh(a_{j_k} \tau_j)$ and hence the interaction time interval is given by $(2/a_{j_k}) \tanh^{-1}(v_j)$. So the integration limits are from $-\mathcal{T}_{j_k}/2$ to $\mathcal{T}_{j_k}/2$.

However, evaluation of the integrations, appearing in $\Delta\mathcal{P}_j$ and $\Delta\mathcal{P}_{AB}$, for finite integration limits can not be done analytically. But a suitable choice of a switching function $\chi_j(\tau_j)$, which vanishes rapidly beyond the finite integration limits, can allow to extend the interaction time limits from $-\infty$ to $+\infty$. In that case there is a possibility of obtaining an analytical expression. Following the argument of [12] and as suggested there (later used in [13] as well), we choose a Lorentzian like compact symmetric switching function:

$$\chi_j(\tau_j) = \frac{(\mathcal{T}_{j_k}/2)^2}{\tau_j^2 + (\mathcal{T}_{j_k}/2)^2}. \quad (20)$$

This function is non-vanishing for $-\mathcal{T}_{j_k}/2 < \tau_j < \mathcal{T}_{j_k}/2$, and approximately zero beyond this domain. We could choose a Gaussian like switching function [12], however that will not help us to extend the integration limit from $\pm\mathcal{T}_{j_k}/2$ to $\pm\infty$. Because at $\tau_j \rightarrow i \times \infty$, the gaussian exponent ($\exp(-\tau_j^2/\mathcal{T}_{j_k}^2)$) diverges and that fails Jordan's lemma for contour integration.

3.1 Both detectors are moving parallelly

The two qubits (the detectors here) are accelerating with constant accelerations (a_{H_A} and a_{H_B}) in the RRW during the second stage of the cycle. In this case their trajectories are given by (18) and the relation between the proper times between them turns out to be (from (A.2), see also [17])

$$\tau_B = \alpha_{a_H} \tau_A, \quad (21)$$

where $\alpha_{a_H} = a_{A_H}/a_{B_H}$ (since this is the heating stage). Using the switching function (20) and extending the limits of integration from $-\infty$ to $+\infty$ in (15) and (17), one can perform the integrations analytically. In the evaluation of these, since here our designated observer's frame is qubit A , all the integration variables will be expressed in terms of τ_A by using (21).

The explicit calculations for \mathcal{P}_A and \mathcal{P}_B are presented in Appendix D. The values of these quantities are given by

$$\begin{aligned} \mathcal{P}_A(\omega_2) &= \frac{(a_{A_H} \mathcal{T}_{A_H}/2)^2 e^{-\mathcal{T}_{A_H} \omega_2}}{16 \sin^2(a_{A_H} \mathcal{T}_{A_H}/2)} \\ &+ \frac{a_{A_H}^2 \mathcal{T}_{A_H}^2 e^{-\frac{2\pi\omega_2}{a_{A_H}}}}{64\pi^2} \left(\Phi \left(e^{-\frac{2\pi\omega_2}{a_{A_H}}}, 2, 1 + \frac{a_{A_H} \mathcal{T}_{A_H}}{2\pi} \right) - \Phi \left(e^{-\frac{2\pi\omega_2}{a_{A_H}}}, 2, 1 - \frac{a_{A_H} \mathcal{T}_{A_H}}{2\pi} \right) \right) \\ &+ \frac{a_{A_H} \mathcal{T}_{A_H}^2 \omega_2 e^{-\frac{2\pi\omega_2}{a_{A_H}}}}{32\pi} \left(\Phi \left(e^{-\frac{2\pi\omega_2}{a_{A_H}}}, 1, 1 + \frac{a_{A_H} \mathcal{T}_{A_H}}{2\pi} \right) - \Phi \left(e^{-\frac{2\pi\omega_2}{a_{A_H}}}, 1, 1 - \frac{a_{A_H} \mathcal{T}_{A_H}}{2\pi} \right) \right), \end{aligned} \quad (22)$$

$$\mathcal{P}_A(-\omega_2) = \frac{\omega_2 \mathcal{T}_{A_H}}{8} + \mathcal{P}_A(\omega_2); \quad \Delta\mathcal{P}_A(\omega_2) = \mathcal{P}_A(\omega_2) - \mathcal{P}_A(-\omega_2) \quad (23)$$

$$\begin{aligned} \mathcal{P}_B(\omega_2) &= \frac{(a_{A_H} \mathcal{T}_{A_H}/2)^2 e^{-\mathcal{T}_{A_H} \alpha_{a_H} \omega_2}}{16 \sin^2(a_{A_H} \mathcal{T}_{A_H}/2)} \\ &+ \frac{a_{A_H}^2 \mathcal{T}_{A_H}^2 e^{-\frac{2\pi\omega_2}{a_{B_H}}}}{64\pi^2} \left(\Phi \left(e^{-\frac{2\pi\omega_2}{a_{B_H}}}, 2, 1 + \frac{a_{A_H} \mathcal{T}_{A_H}}{2\pi} \right) - \Phi \left(e^{-\frac{2\pi\omega_2}{a_{B_H}}}, 2, 1 - \frac{a_{A_H} \mathcal{T}_{A_H}}{2\pi} \right) \right) \\ &+ \frac{a_{A_H} \mathcal{T}_{A_H}^2 \alpha_{a_H} \omega_2 e^{-\frac{2\pi\omega_2}{a_{B_H}}}}{32\pi} \left(\Phi \left(e^{-\frac{2\pi\omega_2}{a_{B_H}}}, 1, 1 + \frac{a_{A_H} \mathcal{T}_{A_H}}{2\pi} \right) - \Phi \left(e^{-\frac{2\pi\omega_2}{a_{B_H}}}, 1, 1 - \frac{a_{A_H} \mathcal{T}_{A_H}}{2\pi} \right) \right), \end{aligned} \quad (24)$$

and

$$\mathcal{P}_B(-\omega_2) = \frac{\mathcal{T}_{A_H} \omega_2 \alpha_{a_H}}{8} + \mathcal{P}_B(\omega_2); \quad \Delta\mathcal{P}_B(\omega_2) = \mathcal{P}_B(\omega_2) - \mathcal{P}_B(-\omega_2) \quad (25)$$

In the above, Φ is the transcendental Lerch-Hurwitz function, defined as

$$\Phi(z, s, a) = \sum_{k=0}^{\infty} \frac{z^k}{(k+a)^s}. \quad (26)$$

Similarly $\Delta\mathcal{P}_{AB}$ has been calculated in Appendix E.1. We obtain \mathcal{P}_{AB} for $\alpha_{a_H} < 1$ case as

$$\Delta\mathcal{P}_{AB} = -\frac{\alpha_{a_H} a_{B_H} \mathcal{T}_{A_H}^3 \operatorname{csch}(a_{A_H} \kappa) e^{-\frac{1}{2}(1-\alpha_{a_H})\mathcal{T}_{A_H}\omega_2}}{16 \kappa (\kappa^2 + \mathcal{T}_{A_H}^2)} (\kappa \sin(\alpha_{a_H} \kappa \omega_2) + \kappa \sin(\kappa \omega_2) + \mathcal{T}_{A_H} \cos(\alpha_{a_H} \kappa \omega_2) - \mathcal{T}_{A_H} \cos(\kappa \omega_2)), \quad (27)$$

while that for $\alpha_{a_H} > 1$ case is

$$\Delta\mathcal{P}_{AB} = -\frac{\alpha_{a_H} a_{B_H} \mathcal{T}_{A_H}^3 \operatorname{csch}(a_{A_H} \kappa) e^{-\frac{1}{2}(\alpha_{a_H}-1)\mathcal{T}_{A_H}\omega_2}}{16 \kappa (\kappa^2 + \mathcal{T}_{A_H}^2)} (\kappa \sin(\alpha_{a_H} \kappa \omega_2) + \kappa \sin(\kappa \omega_2) - \mathcal{T}_{A_H} \cos(\alpha_{a_H} \kappa \omega_2) + \mathcal{T}_{A_H} \cos(\kappa \omega_2)). \quad (28)$$

Here κ is defined through the relation $\cosh(a_{A_H} \kappa) = (a_{A_H}/a_{B_H} + a_{B_H}/a_{A_H})/2$. Here it should be pointed out that for $\alpha_a = 1$, both expressions of \mathcal{P}_{AB} and $\Delta\mathcal{P}_B$, given in (27), (28) and (25) will be reduced to $\Delta\mathcal{P}_A$ given in (23). Thus for $\alpha_{a_H} = 1$, values of the trace quantities corresponding to work done and heat absorbed by the system are always *zero* and *negative* for initial maximally anti-symmetric and maximally symmetric entangled states, respectively (due to (14) and (23)). Thus for $\alpha_{a_H} = 1$, condition (11) does not get satisfied for maximally entangled states.

For the qualitative analysis of the above results we will need the above expressions in terms of scaled dimensionless parameters. If we define the dimensionless quantities as $a_{A_H} \mathcal{T}_{A_H} (= \mathcal{A})$, $a_{B_H} \mathcal{T}_{A_H} (= \mathcal{B} = \mathcal{A}/\alpha_{a_H})$, $\omega_2 \mathcal{T}_{A_H} (= \mathcal{W})$ and $\kappa/\mathcal{T}_{A_H} (= \mathcal{X})$, one can check that \mathcal{P}_A , \mathcal{P}_B and $\Delta\mathcal{P}_{AB}$ are all dimensionless quantities. In terms of these one finds

$$\begin{aligned} \mathcal{P}_A(\mathcal{W}) &= \frac{(\mathcal{A}/2)^2 e^{-\mathcal{W}}}{16 \sin^2(\mathcal{A}/2)} + \frac{\mathcal{A}^2 e^{-\frac{2\pi\mathcal{W}}{\mathcal{A}}}}{64\pi^2} \left(\Phi\left(e^{-\frac{2\pi\mathcal{W}}{\mathcal{A}}}, 2, 1 + \frac{\mathcal{A}}{2\pi}\right) - \Phi\left(e^{-\frac{2\pi\mathcal{W}}{\mathcal{A}}}, 2, 1 - \frac{\mathcal{A}}{2\pi}\right) \right) \\ &+ \frac{\mathcal{A}\mathcal{W} e^{-\frac{2\pi\mathcal{W}}{\mathcal{A}}}}{32\pi} \left(\Phi\left(e^{-\frac{2\pi\mathcal{W}}{\mathcal{A}}}, 1, 1 + \frac{\mathcal{A}}{2\pi}\right) - \Phi\left(e^{-\frac{2\pi\mathcal{W}}{\mathcal{A}}}, 1, 1 - \frac{\mathcal{A}}{2\pi}\right) \right), \end{aligned} \quad (29)$$

$$\begin{aligned} \mathcal{P}_B(\mathcal{W}) &= \frac{(\mathcal{A}/2)^2 e^{-\alpha_{a_H}\mathcal{W}}}{16 \sin^2(\mathcal{A}/2)} + \frac{\mathcal{A}^2 e^{-\frac{2\pi\mathcal{W}\alpha_{a_H}}{\mathcal{A}}}}{64\pi^2} \left(\Phi\left(e^{-\frac{2\pi\mathcal{W}\alpha_{a_H}}{\mathcal{A}}}, 2, 1 + \frac{\mathcal{A}}{2\pi}\right) - \Phi\left(e^{-\frac{2\pi\mathcal{W}\alpha_{a_H}}{\mathcal{A}}}, 2, 1 - \frac{\mathcal{A}}{2\pi}\right) \right) \\ &+ \frac{\mathcal{A}\mathcal{W}\alpha_{a_H} e^{-\frac{2\pi\mathcal{W}\alpha_{a_H}}{\mathcal{A}}}}{32\pi} \left(\Phi\left(e^{-\frac{2\pi\mathcal{W}\alpha_{a_H}}{\mathcal{A}}}, 1, 1 + \frac{\mathcal{A}}{2\pi}\right) - \Phi\left(e^{-\frac{2\pi\mathcal{W}\alpha_{a_H}}{\mathcal{A}}}, 1, 1 - \frac{\mathcal{A}}{2\pi}\right) \right), \end{aligned} \quad (30)$$

$$\mathcal{P}_B(-\mathcal{W}) = \frac{\mathcal{W}\alpha_{a_H}}{8} + \mathcal{P}_B(\mathcal{W}); \quad \mathcal{P}_A(-\mathcal{W}) = \frac{\mathcal{W}}{8} + \mathcal{P}_A(\mathcal{W}), \quad (31)$$

$$\Delta\mathcal{P}_{AB} = -\frac{\alpha_{a_H} \mathcal{B} \operatorname{csch}(\mathcal{X}\mathcal{K}) e^{-\frac{1}{2}(1-\alpha_{a_H})\mathcal{W}}}{16 \mathcal{X} (\mathcal{X}^2 + 1)} (\mathcal{X} \sin(\alpha_{a_H} \mathcal{X}\mathcal{W}) + \mathcal{X} \sin(\mathcal{X}\mathcal{W}) + \cos(\alpha_{a_H} \mathcal{X}\mathcal{W}) - \cos(\mathcal{X}\mathcal{W})), \quad (32)$$

for $\alpha_{a_H} < 1$ and

$$\Delta\mathcal{P}_{AB} = -\frac{\alpha_{a_H} \mathcal{B} \operatorname{csch}(\mathcal{X}\mathcal{K}) e^{-\frac{1}{2}(\alpha_{a_H}-1)\mathcal{W}}}{16 \mathcal{X} (\mathcal{X}^2 + 1)} (\mathcal{X} \sin(\alpha_{a_H} \mathcal{X}\mathcal{W}) + \mathcal{X} \sin(\mathcal{X}\mathcal{W}) - \cos(\alpha_{a_H} \mathcal{X}\mathcal{W}) + \cos(\mathcal{X}\mathcal{W})), \quad (33)$$

for $\alpha_{a_H} > 1$. Using these quantities, the required expression (14) need to be evaluated to determine the efficiency. Below we will analyse the final expressions for initial state, $b_1|e_A g_B\rangle + b_2|g_A e_B\rangle$ with different values of b_1 and b_2 (under the constraint $b_1^2 + b_2^2 = 1$), separately.

3.1.1 Analysis for maximally entangled symmetrical initial state

Here, we have $b_1 = b_2 = 1/\sqrt{2}$. From (23) and (25) we know that $\Delta\mathcal{P}_A(\omega)$ and $\Delta\mathcal{P}_B(\omega)$ are always negative quantity. Constructing a Otto cycle requires, $\text{Tr}(\delta\rho^H h_{\alpha_v})$, $\text{Tr}(\delta\rho^H h_{\alpha_{a_H}})$ and $\text{Tr}(\delta\rho^H h_{\alpha_{a_C}})$ need to be positive for some values of \mathcal{A} , $\mathcal{B}(= \mathcal{A}/\alpha_a)$, \mathcal{W} , α_{a_C} . We find that $\text{Tr}(\delta\rho^H h_{\alpha_v})$ is always negative in the parameter space (for instance, see Fig. 1) for both the cases ($\alpha_a < 1$ and $\alpha_a > 1$). This implies that

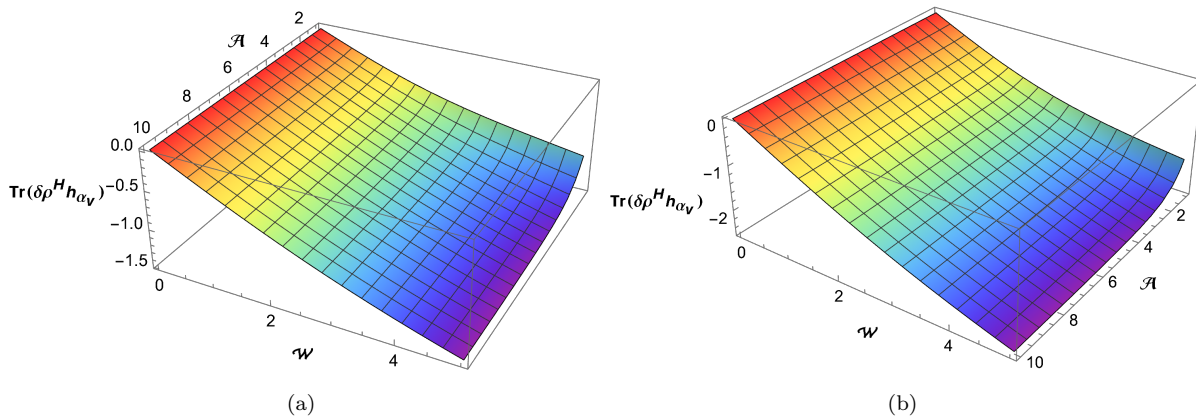


Figure 1: Initial state $|s\rangle$ for parallel motion: Plots (a) and (b) show trace corresponding to work done by the system, $\text{Tr}(\delta\rho^H h_{\alpha_v})$ with respect to dimensionless acceleration of the primary detector (\mathcal{A}) and dimensionless energy gap (\mathcal{W}) of the composite system for $\alpha_{a_H} = 0.5$ and $\alpha_{a_H} = 1.5$, respectively.

condition (11) is always violated and hence no EUQOE can be made up with two initially symmetric maximally entangled detectors moving in parallel motion.

3.1.2 Analysis for maximally entangled anti-symmetrical initial state

As mentioned earlier, a successful Otto cycle can be built, provided the condition (11) is being satisfied. Therefore, satisfaction of this condition determine the parameter space for the available quantities which are involved in constructing the cycle. In order to do that we have plotted dimensionless quantity $\text{Tr}(\delta\rho^H h_{\alpha_v})$ in Fig. 2, with respect to dimensionless quantities \mathcal{A} , \mathcal{W} with fixed α_a values ($\alpha_a = 0.5$ and $\alpha_a = 1.5$, respectively). The 3D plots are showing that there are no positive values of $\text{Tr}(\delta\rho^H h_{\alpha_v})$ for

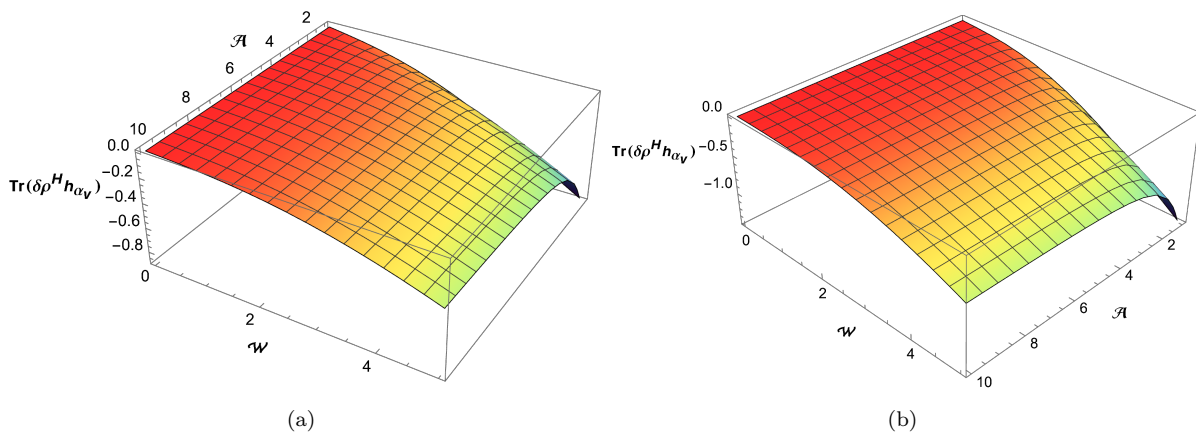


Figure 2: Initial state $|a\rangle$ for parallel motion: Plots (a) and (b) show trace corresponding to work done by the system, $\text{Tr}(\delta\rho^H h_{\alpha_v})$ with respect to dimensionless acceleration of the primary detector (\mathcal{A}) and dimensionless energy gap (\mathcal{W}) of the composite system for $\alpha_{a_H} < 1$ (here $\alpha_{a_H} = 0.5$) and $\alpha_{a_H} > 1$ (here $\alpha_{a_H} = 1.5$), respectively.

any \mathcal{A} and \mathcal{W} . Thus making of Entangled Otto cycle is not possible in this case.

3.1.3 Analysis for non-maximally entangled initial state

The initial state for $b_2 \neq 1/\sqrt{2}$ with $|b_1|^2 + |b_2|^2 = 1$, gives several choices for non-maximally entangled state where $0 < b_2 < 1$ (except $b_2 \neq 1/\sqrt{2}$). In Fig. 3, we have plotted $\text{Tr}(\delta\rho^H h_{\alpha_v})$ with respect to \mathcal{A} and \mathcal{W} for values $\alpha_a = 0.2, 1.0, 1.2$. We used $|b_2| = 0.9$ with b_1 and b_2 having same or different signs. We have scanned the parameter space for different values of b_2 and α_a , but found no region where any of the trace quantities satisfy the condition given by (11). Hence, making of EUQOE is not possible for any entangled initial state, while the detectors are in parallel motion.

3.2 The detectors are moving anti-parallelly:

In this case detector A is moving in RRW while other one (i.e. B) is moving in LRW during the accelerated phase. In this case trajectories of detector A and detector B are given by (18) and (19), respectively. The relation between the proper times of the detectors is given by (from (A.4))

$$\tau_B = -\alpha_{a_H} \tau_A \quad (34)$$

Using this relation, \mathcal{P}_A , \mathcal{P}_B and \mathcal{P}_{AB} are calculated in terms of the proper time of the detector A . Expressions of \mathcal{P}_A are already presented in (22) and (23). In Appendix D, we obtain expressions of \mathcal{P}_B when the detector B is accelerating in LRW. These are found to be same in value for the detector is accelerating in RRW. Therefore these are given by (24) and (25). In Appendix E.2, we obtain $\Delta\mathcal{P}_{AB} = \mathcal{P}_{AB}(\omega, -\omega) - \mathcal{P}_{AB}(-\omega, \omega)$ for all α_a values as

$$\Delta\mathcal{P}_{AB} = 0 . \quad (35)$$

Therefore, for anti-parallel motion, trace quantities get simplified and expressions are same for any value of α_a . The relative sign between b_1 and b_2 will not matter for anti-parallel motion of the detectors (see (14)).

3.2.1 Analysis for maximally symmetric and anti-symmetric entangled initial state

For the maximally entangled state *i.e.*, $|b_1|^2 = |b_2|^2 = 1/2$, we have

$$\Delta\mathcal{P}_A = -\frac{\mathcal{W}}{8}; \quad \Delta\mathcal{P}_B = -\frac{\alpha_{a_H} \mathcal{W}}{8} = \alpha_{a_H} \Delta\mathcal{P}_A , \quad (36)$$

Therefore from (14), we can conclude that work done or heat absorption are same for both symmetric and anti-symmetric initial states. For total work done, $\alpha = \alpha_v = 1/\gamma$ is the inverse Lorentz factor, which is always positive. The trace corresponding to total work done by the system can be calculated from (14), given by

$$\text{Tr}(\delta^H h_{\alpha_v}) = [\Delta\mathcal{P}_A + \alpha_v \Delta\mathcal{P}_B] = (1 + \alpha_v \alpha_{a_H}) \Delta\mathcal{P}_A \quad (37)$$

and the trace corresponding to heat absorbed by the system is

$$\text{Tr}(\delta^H h_{\alpha_{a_H}}) = [\Delta\mathcal{P}_A - \alpha_{a_H} \Delta\mathcal{P}_B] = (1 - \alpha_{a_H}^2) \Delta\mathcal{P}_A . \quad (38)$$

Here, we can immediately see that the work done by the system is always negative due to (36). Therefore, we can not make an Otto cycle in this scenario.

3.2.2 Analysis for non-maximally entangled initial state

In this case (14) reduces to

$$\text{Tr}(\delta\rho^H h_{\alpha_v}) = \{b_2^2 \mathcal{P}_A(\omega) - b_1^2 \mathcal{P}_A(-\omega)\} + \alpha_v \{b_1^2 \mathcal{P}_B(\omega) - b_2^2 \mathcal{P}_B(-\omega)\} . \quad (39)$$

$$\text{Tr}(\delta\rho^H h_{\alpha_{a_H}}) = \{b_2^2 \mathcal{P}_A(\omega) - b_1^2 \mathcal{P}_A(-\omega)\} - \alpha_{a_H} \{b_1^2 \mathcal{P}_B(\omega) - b_2^2 \mathcal{P}_B(-\omega)\} . \quad (40)$$

Here $\alpha = \alpha_v = \sqrt{1 - v_{rel}^2}$ for work done, where by using (18) and (19), one can find $v_{rel} = -2 \tanh(\mathcal{A}) / (1 + \tanh^2(\mathcal{A}))$. For heating stage, we have $\alpha = -\alpha_{a_H}$. In sub-figure (a) and (b) of Fig. 4, we find that for

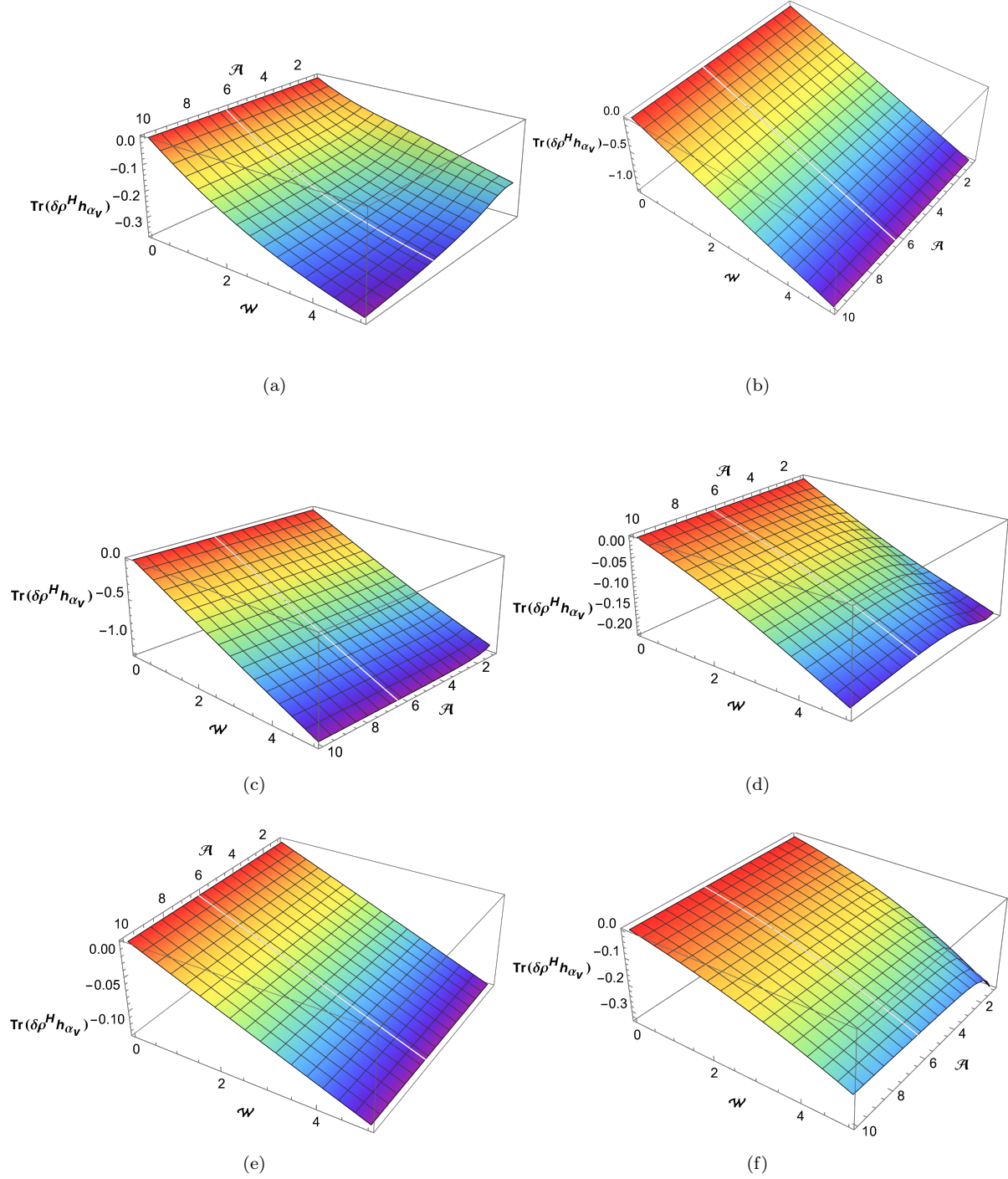


Figure 3: The traces corresponding to work done by the system, $\text{Tr}(\delta\rho^H h_{\alpha_v})$ are plotted with respect to dimensionless acceleration of the primary detector (\mathcal{A}) and dimensionless energy gap (\mathcal{W}) of the composite system for detectors' non-maximally entangled initial state in parallel motion: Plots (a), (b) and (c) are showing the same with $b_1 = b_2 = 0.9$ for $\alpha_{aH} = 0.2, 1.0, 1.2$, respectively. Plots (d), (e) and (f) are showing the same with $b_1 = -b_2 = 0.9$ for $\alpha_{aH} = 0.2, 1.0, 1.2$, respectively.

some fixed b_2 and α_{aH} , $\text{Tr}(\delta\rho^H h_{\alpha_{aH}})$ and $\text{Tr}(\delta\rho^H h_{\alpha_v})$ can be positive within a range of values of \mathcal{A} and \mathcal{W} . We also need to ensure that $\text{Tr}(\delta\rho^H h_{\alpha_{aC}})$ is positive, which is necessary in order to happening of the heat rejection by the cycle in the cooling process. Otherwise, the efficiency of the cycle will be greater

than one. This can be checked from (12), which states that for $\text{Tr}(\delta\rho^H h_{\alpha_{a_C}}) < 0$, $(\omega_2 - \omega_1)\text{Tr}(\delta\rho^H h_{\alpha_v})$ will be greater than $\omega_2\text{Tr}(\delta\rho^H h_{\alpha_{a_H}})$, and in that case one will have $\eta_E > 1$ (see, expression of η_E in (13)). As stated earlier, such is not physically possible. We know that velocity of j -th detector ($j = A, B$) at the start and end of the stage II ($-\mathcal{T}_{jH}/2$ and $\mathcal{T}_{jH}/2$) is same as that at the end and start of the stage IV ($\mathcal{T}_{jC}/2$ and $-\mathcal{T}_{jC}/2$). Using this fact, the following relations can be obtained:

$$a_{AC}\mathcal{T}_{AC} = -a_{AH}\mathcal{T}_{AH} ; \quad (41)$$

$$a_{BC}\mathcal{T}_{BC} = -a_{BH}\mathcal{T}_{BH} ; \quad (42)$$

and

$$\alpha_{a_C}\mathcal{T}_{AC} = \mathcal{T}_{BC} . \quad (43)$$

Here α_{a_C} is given by a_{AC}/a_{BC} . In (41) and (42) as the parameters in the heating process (stage II) are already fixed, we can always freely choose a_{jC} . Note that Eq. (43) can be obtained by taking ratio between (41) and (42) and then using (21). Therefore, any two parameters can be chosen freely and then the third parameter is determined. Here we fix α_{a_C} and \mathcal{T}_{AC} (\mathcal{T}_{BC} will be automatically determined) such that $\text{Tr}(\delta\rho^H h_{\alpha_{a_C}}) > 0$. Now a sufficient condition for satisfaction of energy conservation (from (12)) can be taken as

$$\frac{\mathcal{W}}{\omega_1\mathcal{T}_{AH}}(\alpha_{a_H} - 1) = (\alpha_{a_C} - 1) . \quad (44)$$

Since the values of \mathcal{W} and α_{a_H} are already determined by considering positivity of $\text{Tr}(\delta\rho^H h_{\alpha_v})$ and $\text{Tr}(\delta\rho^H h_{\alpha_{a_H}})$, while α_{a_C} in (43) is chosen to be free, the above equation can fix the value of dimensionless energy gap $\omega_1\mathcal{T}_{AH}$ for $\alpha_{a_C} \neq 1$. In this connection remember that ω_1 is always need to be less than ω_2 . So we have to choose α_{a_C} such that $\omega_1 < \omega_2$ and (44) are satisfied simultaneously. One can notice that ω_1 is positive, if we choose $\alpha_{a_C} > 1$ ($\alpha_{a_C} < 1$) for $\alpha_{a_H} > 1$ ($\alpha_{a_H} < 1$). It should be pointed out that for $\alpha_{a_H} = 1$, we obtain $\omega_1 = 0$ (for $\alpha_{a_C} \neq 1$) or any value of ω_1 (for $\alpha_{a_C} = 1$). However, we will not consider $\omega_1 = 0$ case, as this implies that at the beginning of stage I, energy gap of the system is zero. If we choose $\alpha_{a_H} = 1$ then we also need to choose $\alpha_{a_C} = 1$. For other values of α_{a_H} in detector's anti-parallel motion with non-maximally entangled case, we can always choose α_{a_C} such that $\omega_1 < \omega_2$ and $\text{Tr}(\delta\rho^H h_{\alpha_{a_C}}) > 0$ along with the energy conservation relation satisfied. In sub-figure (c) of Fig. 4 we find that $\text{Tr}(\delta\rho^H h_{\alpha_{a_C}})$ has positive values within a range of values of \mathcal{A} and \mathcal{W} . In this case since we took $\alpha_{a_C} = 0.1$, Eq. (44) implies $\omega_1 < \omega_2$ (as we took $\alpha_{a_H} = 0.2$). In sub-figure (d) of Fig. 4, we have plotted $\text{Tr}(\delta\rho^H h_{\alpha_v})$, $\text{Tr}(\delta\rho^H h_{\alpha_{a_H}})$, $\text{Tr}(\delta\rho^H h_{\alpha_{a_C}})$ and η/η_0 as a function of \mathcal{A} with $\mathcal{W} = 0.2$, $\alpha_{a_H} = 0.2$, $\alpha_{a_C} = 0.1$ and $|b_2| = 0.9$. One can observe that for $\mathcal{A} < 0.33$ (in the gray region), our $\text{Tr}(\delta\rho^H h_{\alpha_v})$ has negative values for these fixed values of parameters. Therefore the Otto cycle is only possible for $\mathcal{A} > 0.33$ for this case. One can also notice that η/η_0 varies with the detectors' acceleration (\mathcal{A}) for fixed values of other parameters and always less than one. Thus even though construction of the entangled Otto cycle is possible, enhancement of efficiency of the cycle is not possible.

Now we aim to investigate how much deviation from maximally entangled state is needed in order to construct a EUQOE. In Fig. 5 we have plotted the trace quantities with respect to b_2 for different values of α_{a_H} . The positivity of the trace quantity related to heat absorption by the system depend on α_{a_H} as indicated by (38). The grey region in the plots represent region with negative traces for given parameter values. In sub-figure (a) (corresponding to $\mathcal{A} = 0.5$) and (b) (for $\mathcal{A} = 5.0$), it is shown that the trace quantity related to heat absorbed by the system is α_{a_H} dependent. Higher the α_{a_H} values, larger the range of b_2 values for which this trace is positive. It should be mentioned that when $\alpha_{a_H} = 1$, $\text{Tr}(\delta\rho^H h_{\alpha_{a_H}})$ is always *zero* for $|b_2| = 1/\sqrt{2}$ (as eq. (40) reduces to $(b_2^2 - b_1^2)[\mathcal{P}_A(\omega) + \mathcal{P}_A(-\omega)]$). For $\alpha_{a_H} > 1$, this quantity also can be positive for $|b_2| < 1/\sqrt{2}$. Same nature will be obtained for $\text{Tr}(\delta\rho^H h_{\alpha_{a_C}})$ along with satisfaction of (44), as only α_{a_H} will be replaced by α_{a_C} . However this will not be useful unless all trace quantities are not positive simultaneously. In sub-figure (c) the trace quantity related to work done by the system is plotted for $\mathcal{A} = 0.5$, which is α_{a_H} dependent, as expected. Higher the α_{a_H} values, smaller the range of b_2 values for which this trace is positive. In sub-figure (d) it is shown that it is almost independent of α_{a_H} for $\mathcal{A} = 5.0$. It is due to the fact that $\alpha_v = \sqrt{1 - v_{rel}^2}$ (with $v_{rel} = -2 \tanh(\mathcal{A})/(1 + \tanh^2(\mathcal{A}))$) get suppressed with higher values of \mathcal{A} .

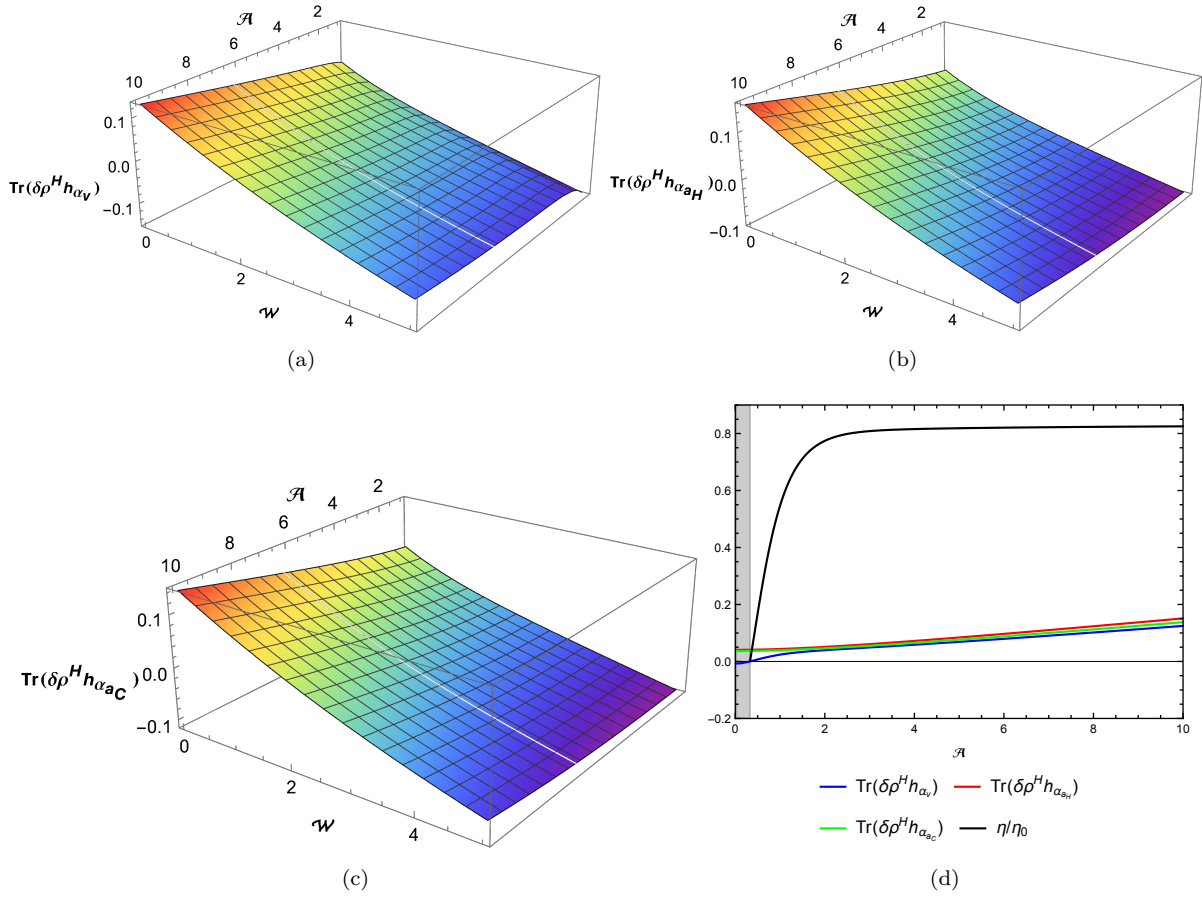


Figure 4: Initially non-maximally entangled state with $|b_2| = 0.9$ for anti-parallel motion: Plots show traces corresponding to (a) work done by the system, $\text{Tr}(\delta\rho^H h_{\alpha_v})$, (b) heat absorbed by the system, $\text{Tr}(\delta\rho^H h_{\alpha_{a_H}})$ with $\alpha_{a_H} = 0.2$ and (c) heat rejected by the system, $\text{Tr}(\delta\rho^H h_{\alpha_{a_C}})$ (we chose $\alpha_{a_C} = 0.1$) with respect to dimensionless acceleration of the primary detector (\mathcal{A}) and dimensionless energy gap (\mathcal{W}) of the composite system. Subfigure (d) shows η/η_0 in black line, $\text{Tr}(\delta\rho^H h_{\alpha_v})$ in blue line, $\text{Tr}(\delta\rho^H h_{\alpha_{a_H}})$ in red line and $\text{Tr}(\delta\rho^H h_{\alpha_{a_C}})$ in green line with respect to dimensionless acceleration of the primary detector (\mathcal{A}) for $\mathcal{W} = 0.2$, $\alpha_{a_H} = 0.2$ and $\alpha_{a_C} = 0.1$. The grey region represent the regime where making of the Otto cycle is not possible.

In sub-figures (a) and (b) of Fig. 6, we have shown the traces corresponding to work done by the system with respect to b_2 for different values of \mathcal{W} (for $\mathcal{A} = 0.5$ and $\mathcal{A} = 10.0$ respectively). Sub-figure (b) shows that for higher \mathcal{A} , $\text{Tr}(\delta\rho^H h_{\alpha_v})$ is *positive* for b_2 is very close to $1/\sqrt{2}$. In sub-figures (c) and (d) of Fig. 6, showing the traces corresponding to heat absorption by the system with respect to b_2 for different values of \mathcal{W} (with $\mathcal{A} = 0.5$ and $\mathcal{A} = 10.0$ respectively). It is visible that $\text{Tr}(\delta\rho^H h_{\alpha_{a_H}})$ is *positive* for $|b_2| < 1/\sqrt{2}$ for $\alpha_{a_H} > 1$. In all the plots in Fig. 6, we choose $\alpha_{a_H} = 2$. Same is drawn for $\alpha_{a_H} = 0.2$ in Fig. 7. All plots are showing that larger the value of \mathcal{W} , smaller the range of b_2 , for which the traces corresponding to work done by the system are positive. Additionally when $\alpha_{a_H} > 1$, the region of b_2 for which the traces corresponding to heat absorbed by the system are positive will be larger as \mathcal{W} increases. Whereas for $\alpha_{a_H} < 1$ the same will be smaller as \mathcal{W} increases. However, since making of EUOE is only possible for a parameter space where all trace quantities are positive simultaneously, therefore we will consider a common parameter space from these figures where all the traces are positive. Here we can see that even though the construction of Otto cycle is not possible for maximally entangled state, but a small deviation form the maximally entangled state can allow us to construct an Otto cycle.

As shown in Figs. 6 and 7, depending upon the given parameters $\text{Tr}(\delta\rho^H h_{\alpha_{a_H}})$ can be *positive* for $b_2 < 1/\sqrt{2}$ or b_2 slightly *greater than* $1/\sqrt{2}$. However $\text{Tr}(\delta\rho^H h_{\alpha_v})$ is *positive* for b_2 is *greater than* $1/\sqrt{2}$. Therefore for these given parameters the making of Otto cycle is possible only when one is away from

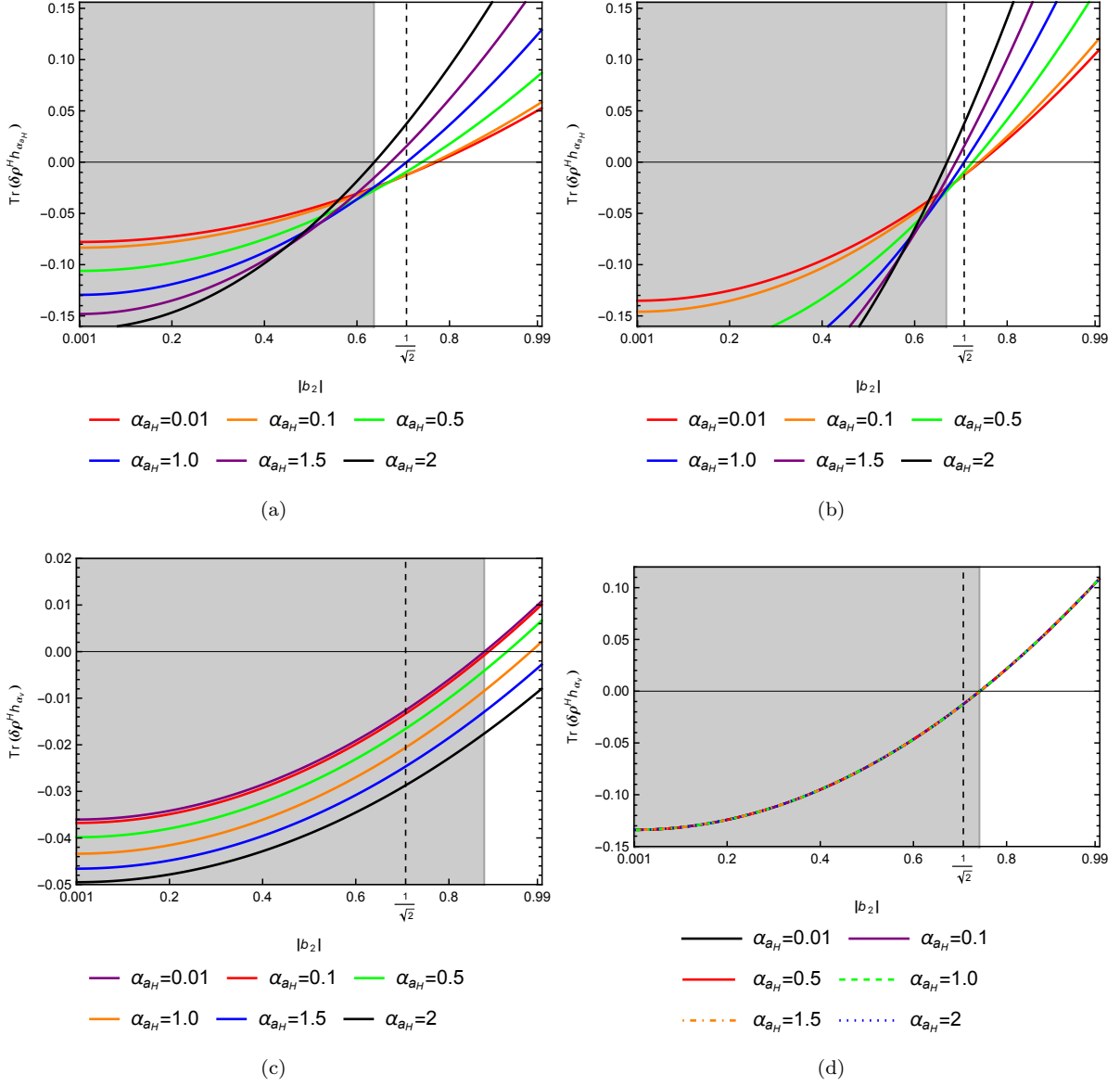


Figure 5: Initially non-maximally entangled state for anti-parallel motion (with fixed $\mathcal{W} = 0.2$): Plots (a) and (b) are showing traces corresponding to heat absorbed by the system, $\text{Tr}(\delta\rho^H h_{\alpha_{a_H}})$ with respect to $|b_2|$ for different α_{a_H} for $\mathcal{A} = 0.5$ and 5.0 , respectively. Plots (c) and (d) are showing traces corresponding to work done by the system, $\text{Tr}(\delta\rho^H h_{\alpha_v})$ with respect to $|b_2|$ for different α_{a_H} for $\mathcal{A} = 0.5$ and 5.0 , respectively. The grey region in the plots roughly represent the regime with negative traces for all given α_{a_H} values.

maximally entangled state. But it may be noticed that larger the value of \mathcal{A} the right side boundary of the shaded region approaching towards $b_2 = 1/\sqrt{2}$ value. Therefore it may appear that a near-maximally entangled state is capable of yielding a Otto cycle. Here we want to estimate such closeness. For higher \mathcal{A} , only the terms in first braces of (39) will dominate. In this situation, $\text{Tr}(\delta\rho^H h_{\alpha_v})$ can be positive for small deviation of b_2 from the maximally entangled case (consider $|b_2| = 1/\sqrt{2} + \epsilon$, with $\epsilon (> 0)$ very small). Then considering upto order ϵ^2 term one finds

$$\begin{aligned}
\text{Tr}(\delta\rho^H h_{\alpha_v}) &= \left(\frac{1}{\sqrt{2}} + \epsilon\right)^2 \mathcal{P}_A(\mathcal{W}) - \left[1 - \left(\frac{1}{\sqrt{2}} + \epsilon\right)^2\right] \mathcal{P}_A(-\mathcal{W}) \\
&\approx \frac{1}{2} \Delta \mathcal{P}_A + \sqrt{2} \epsilon [\mathcal{P}_A(\mathcal{W}) + \mathcal{P}_A(-\mathcal{W})] + \epsilon^2 \mathcal{P}_A(-\mathcal{W}) .
\end{aligned} \tag{45}$$

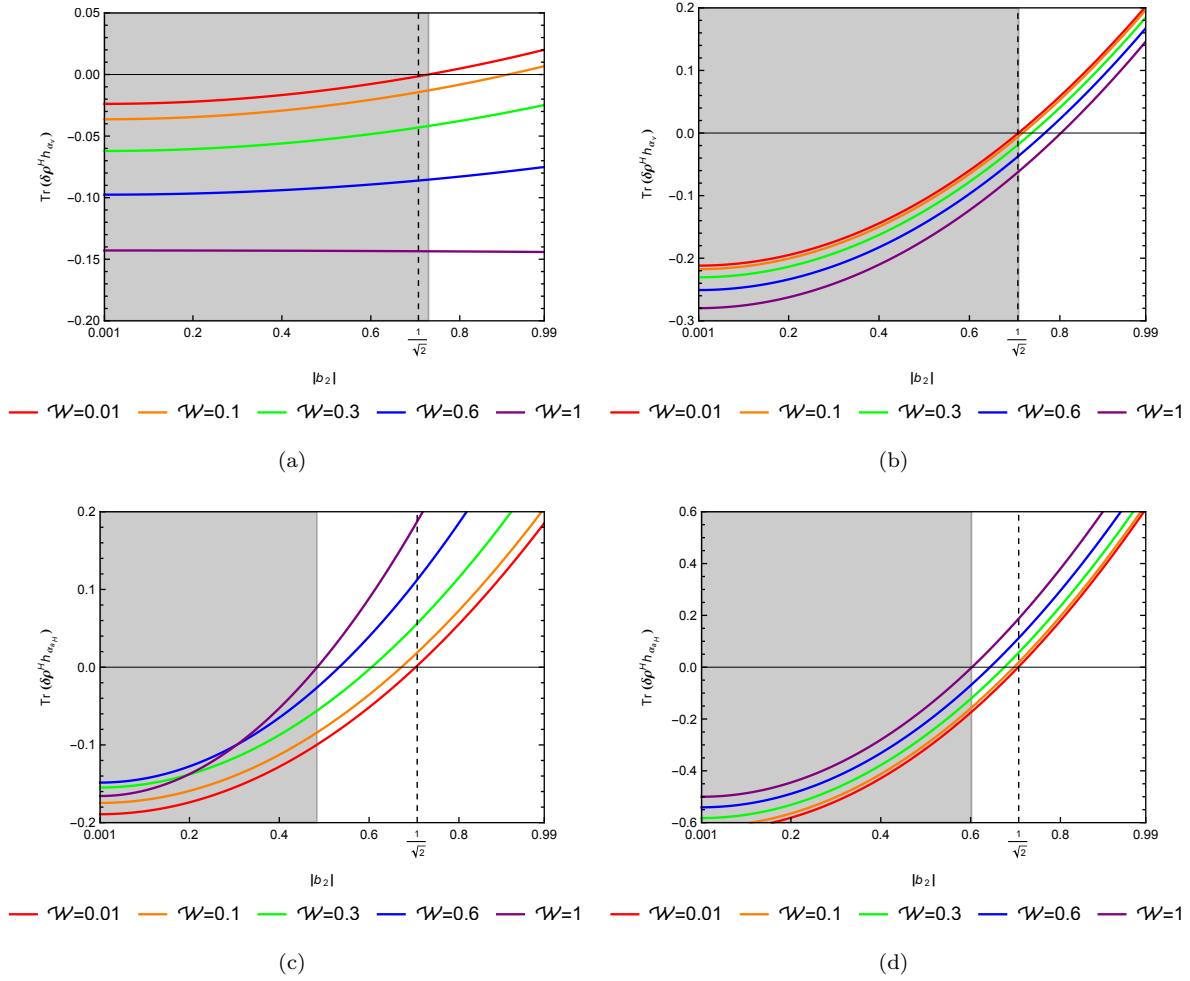


Figure 6: Initially non-maximally entangled state for anti-parallel motion (with fixed $\alpha_{a_H} = 2.0$): Plots (a) and (b) are showing traces corresponding to work done by the system, $\text{Tr}(\delta\rho^H h_{\alpha_v})$ with respect to $|b_2|$ for different dimensionless energy gap (\mathcal{W}) of the composite system for $\mathcal{A} = 0.5$ and $\mathcal{A} = 10.0$, respectively. Plots (c) and (d) are showing traces corresponding to heat absorbed by the system, $\text{Tr}(\delta\rho^H h_{\alpha_H})$ with respect to $|b_2|$ for different dimensionless energy gap (\mathcal{W}) of the composite system for $\mathcal{A} = 0.5$ and $\mathcal{A} = 10.0$, respectively. The grey region in the plots roughly represent the regime with negative traces for given \mathcal{W} values.

Here the first quantity is *negative* and independent of \mathcal{A} (see (31)), but second and third quantities are *positive* (see (29) and (31) for expressions of $\mathcal{P}_A(\mathcal{W})$ and $\mathcal{P}_A(-\mathcal{W})$; which are individually positive quantity and increases with \mathcal{A}). Therefore if at least we have $\epsilon = -\Delta\mathcal{P}_A/(2\sqrt{2}[\mathcal{P}_A(\mathcal{W}) + \mathcal{P}_A(-\mathcal{W})]) \equiv \epsilon_0$, then this trace will be positive. For $\epsilon = \epsilon_0$, first two terms in (45) cancel each other. The remaining term be the third term, which is in the order of ϵ^2 . In Fig. 8, we have plotted $\mathcal{P}_A(\mathcal{W}) + \mathcal{P}_A(-\mathcal{W})$, $\Delta\mathcal{P}_A$ and ϵ_0 with respect to \mathcal{A} . These plots are independent of α_{a_H} . The plot of $\mathcal{P}_A(\mathcal{W}) + \mathcal{P}_A(-\mathcal{W})$ is divided by a numerical factor just for plotting convenience. We can see that ϵ_0 is indeed very small (with $\mathcal{W} = 0.01$ and 0.1, respectively), and decreases more for the higher values of \mathcal{A} where the above estimation can be trusted. Thus, very small ϵ is required for small \mathcal{W} and large \mathcal{A} to make this trace positive. We add a table (Table 1) for values of ϵ_0 and corresponding values of $\text{Tr}(\delta\rho^H h_{\alpha_v})$ from Fig. 8. As the value of \mathcal{A} is increasing, ϵ_0 is getting more smaller. However in this case the values of $\text{Tr}(\delta\rho^H h_{\alpha_v})$ are becoming almost negligible as it is of the order ϵ^2 in this range. The order of magnitude of the numerical values of $\text{Tr}(\delta\rho^H h_{\alpha_v})$ are becoming so small that these fall into the range of noise in the numerical analysis and hence these can not be trusted. Therefore ϵ can not be arbitrarily small in order to satisfy the condition (11) and so the initial entangled state must be “considerable” away (at least in the range of numerical perseverance) from the maximally entangled state in order to make an Otto cycle.

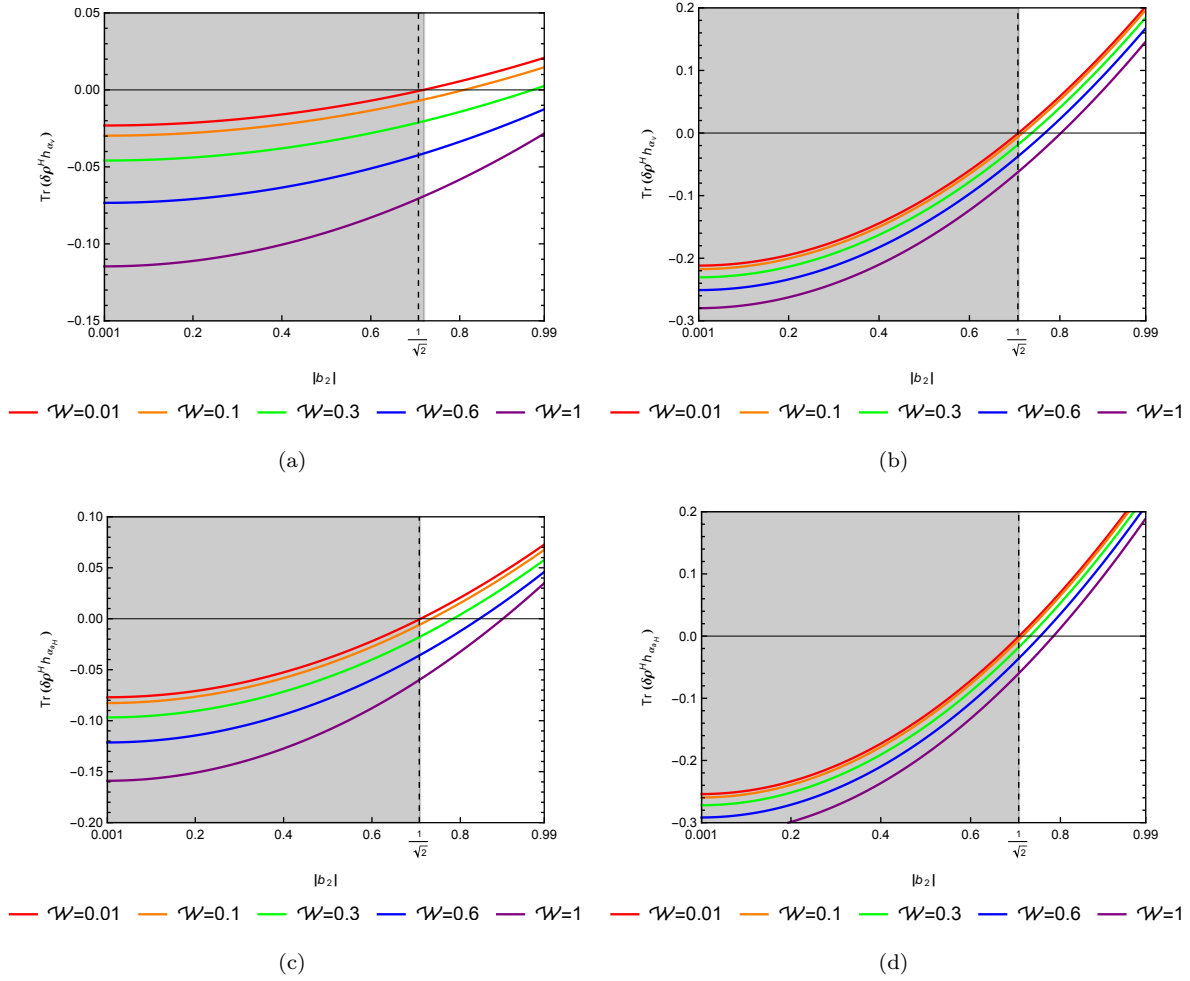


Figure 7: Initially non-maximally entangled state for anti-parallel motion (with fixed $\alpha_{a_H} = 0.2$): Plots (a) and (b) are showing traces corresponding to work done by the system, $\text{Tr}(\delta\rho^H h_{\alpha_v})$ with respect to $|b_2|$ for different values of dimensionless energy gap (\mathcal{W}) of the composite system for $\mathcal{A} = 0.5$ and $\mathcal{A} = 10.0$, respectively. Plots (c) and (d) are showing traces corresponding to heat absorbed by the system, $\text{Tr}(\delta\rho^H h_{\alpha_H})$ with respect to $|b_2|$ for different values of dimensionless energy gap (\mathcal{W}) of the composite system for $\mathcal{A} = 0.5$ and $\mathcal{A} = 10.0$, respectively. The grey region in the plots roughly represent the regime with negative traces for given \mathcal{W} values.

The above analysis, through the figures 5, 6 and 7, provides the space of parameters where our Otto cycle is possible. We will now investigate the nature of efficiency with respect to strength of initial entanglement within these available values of parameters. For this in Fig. 9, we have shown variation of the quantity η/η_0 with respect to b_2 for different values of α_{a_H} with a fixed $\mathcal{W} = 0.2$. Here in sub-figures (a) and (b), we have used $\mathcal{A} = 0.5$ and $\mathcal{A} = 5.0$, respectively. Similarly in Fig. 10, the variation of η/η_0 with respect to b_2 is shown for different values of \mathcal{W} with fixed α_{a_H} values. Here sub-figures (a) and (b) are showing the same with $\alpha_{a_H} = 2.0$ for $\mathcal{A} = 0.5$ and $\mathcal{A} = 10.0$, respectively. Whereas sub-figures (c) and (d) are corresponding to $\alpha_{a_H} = 0.2$ for $\mathcal{A} = 0.5$ and $\mathcal{A} = 10.0$, respectively. All these plots show that the value of η/η_0 is increasing as b_2 is moving away from $b_2 = 1/\sqrt{2}$, but never exceeding *one*. This implies that the efficiency of our EUQOE is always less than that of UQOE. Moreover, this efficiency increases if the initial composite state moves away from the maximally entangled state. Therefore it is likely that “the entanglement suppresses the efficiency of the Otto cycle and as initial entanglement decreases, the efficiency gradually grows”. In addition it is to be observed in Fig. 9 that for a given value of \mathcal{W} the engine is becoming less efficient as relative acceleration α_{a_H} between the detectors increases. Similarly Fig. 10 indicates that for a given α_{a_H} the engine losses its efficiency with the increase of \mathcal{W} .

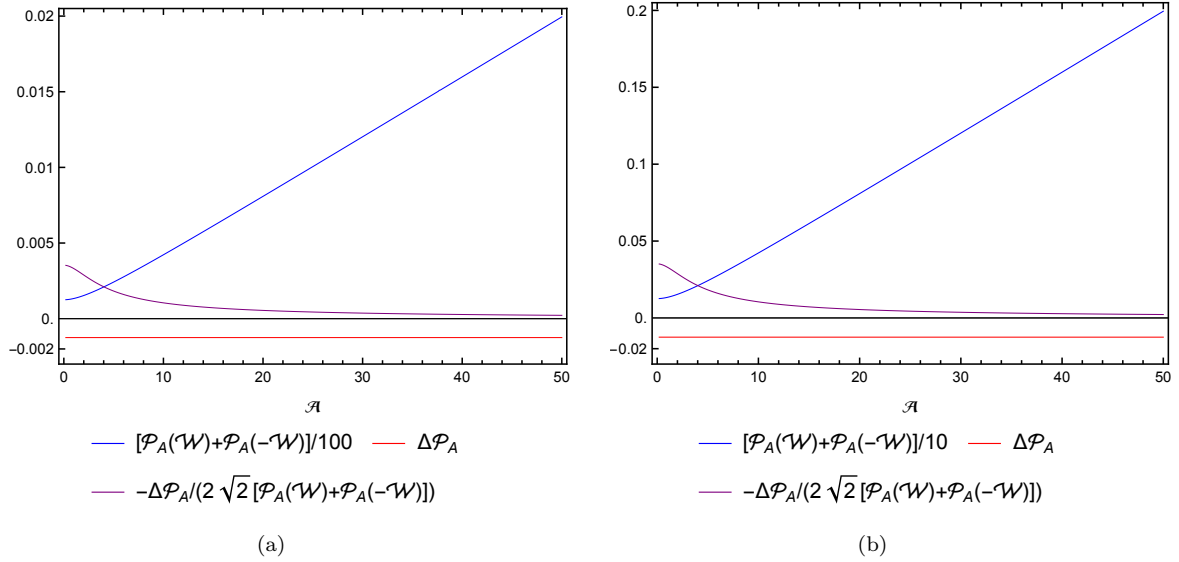


Figure 8: Estimation of ϵ_0 , for (a) $\mathcal{W} = 0.01$ and (b) $\mathcal{W} = 0.1$ (independent of α_{a_H}).

Table 1: The values of ϵ_0 and corresponding values of $\text{Tr}(\delta\rho^H h_{\alpha_v})$ from Fig. 8.

\mathcal{W}	α_{a_H}	\mathcal{A}	ϵ_0	$\text{Tr}(\delta\rho^H h_{\alpha_v})$
0.1	2	10	0.0104596	0.0000462253
	2	20	0.00546493	0.0000241518
	2	30	0.00367563	0.0000162441
	2	40	0.00276543	0.0000122216
	2	50	0.0022156	9.79166×10^{-6}
0.01	2	10	0.00104626	4.62368×10^{-7}
	2	20	0.000546536	2.41537×10^{-7}
	2	30	0.000367576	1.62447×10^{-7}
	2	40	0.000276548	1.22218×10^{-7}
	2	50	0.000221563	9.7918×10^{-8}

4 Conclusion

We have investigated the possibility of construction of a EUQOE with different initial entangled states between two qubits (taken as monopole detectors), which was recently initiated in [15]. The thermal bath has been mimicked by uniformly accelerating the detectors, either in parallel or in anti-parallel motion. As mentioned in the introduction, there were few limitations and incompleteness in the initial attempt. The present discussion raised above those limitations and provided a complete study of constructing a EUQOE.

We found that making of EUQOE is not possible for all cases. There are only one situation when all necessary conditions for making an Otto engine is satisfied. This is when the detectors are in anti-parallel motion with the initial detector's states are non-maximally entangled states. In this case we got some continuous range of values of acceleration of first detector (\mathcal{A}), for some fixed values of the system's energy gap and ratio of the accelerations of the detectors. In the allowed \mathcal{A} range, the efficiency first increasing and then approaching a constant value with respect to \mathcal{A} , however the efficiency never goes beyond η_0 . Thus entangled Otto engines are not fruitful in terms of efficiency of the engine. In other words, the entanglement causes suppression of efficiency. In fact, as the detectors' initial state is approaching towards the maximally entangled state (in allowed b_2 range), efficiency of the cycle deteriorates sharply

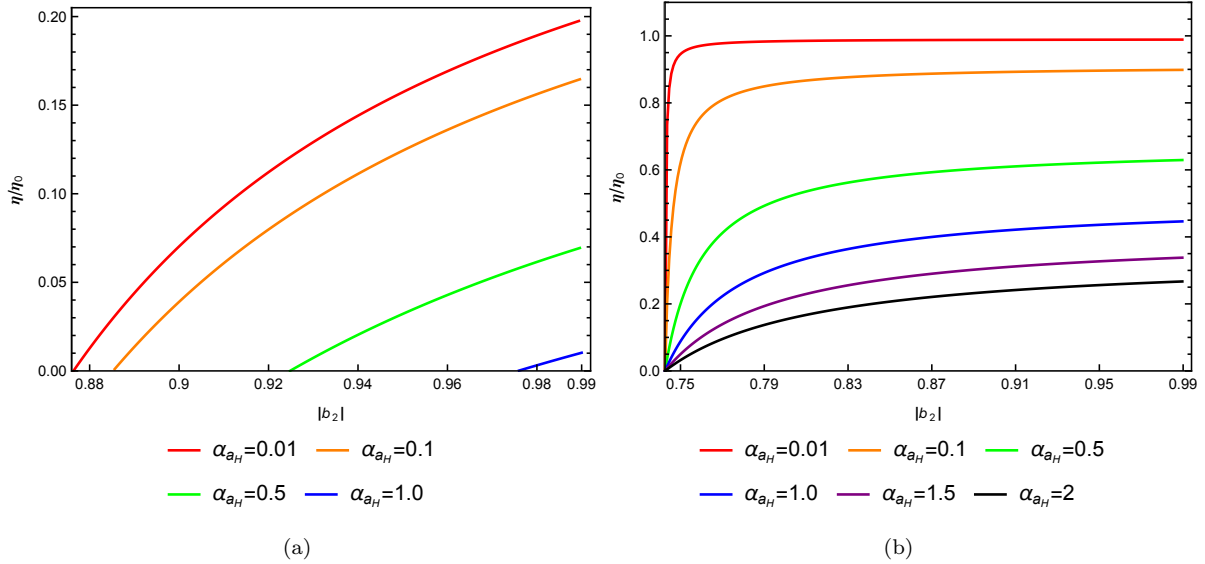


Figure 9: η/η_0 is plotted with respect to $|b_2|$ for different values of α_{a_H} with $\mathcal{W} = 0.2$. Plots (a) and (b) are for $\mathcal{A} = 0.5$ and $\mathcal{A} = 5.0$, respectively.

and becomes *zero*. For all other cases making of EUQOE is not possible. We summarise these outcomes in Table 2.

Table 2: Summery of possible scenarios of EUQOE.

Motion	Initial States	Satisfying all criteria?	Can η/η_0 be greater than one?
Parallel	Maximally entangled, Symmetric	No	-
	Maximally entangled, Anti-symmetric	No	-
	Non-maximally entangled	No	-
Anti-parallel	Maximally entangled, Symmetric	No	-
	Maximally entangled, Anti-symmetric	No	-
	Non-maximally entangled	Yes	No

Couple of comments are in order. In the original QOE, one provides a real thermal bath and therefore the existence of this bath is classical in nature. While our EUQOE (also UQOE, proposed in [12, 13]) is a pure quantum mechanical in construction in the sense that the thermal bath itself is provided through a pure quantum (plus relativistic) effect(s). Finally, it need to be mentioned that the efficiency here can be regulated by changing the observer's acceleration, ratio of detector A to detector B 's acceleration and the energy gap of the detectors' system. Such a unique feature of EUQOE can be very important for experimental verification of the Unruh effect as this phenomenon is the main input in our analysis. In this study we discussed the possible scenario to setup an Otto cycle. We also provided an example range of parameter values where making of Otto cycle is possible. We hope that with the use of those values of the system parameters one will be able to construct an experimental apparatus which will also be able to verify the existence of Unruh phenomenon.

Acknowledgments: DB would like to acknowledge Ministry of Education, Government of India for providing financial support for his research via the PMRF May 2021 scheme. The research of BRM is supported by a START-UP RESEARCH GRANT (No. SG/PHY/P/BRM/01) from the Indian Institute of Technology Guwahati, India and by a Core Research Grant (File no. CRG/2020/000616) from Science and Engineering Research Board (SERB), Department of Science & Technology (DST), Government of India.

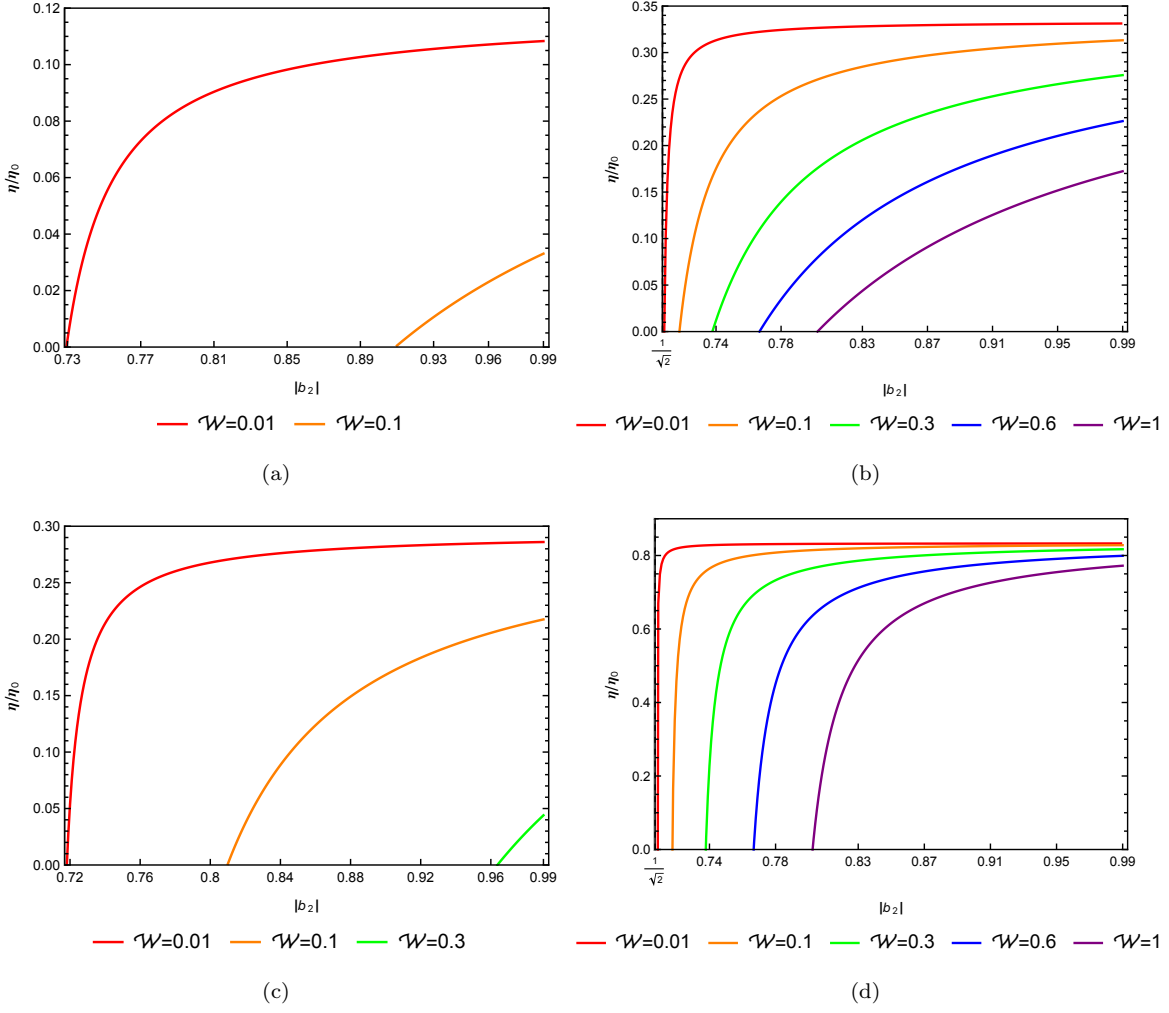


Figure 10: η/η_0 is plotted with respect to $|b_2|$ for different values of \mathcal{W} when the detectors' in anti-parallel motion: For $\alpha_{a_H} = 2.0$, plots (a) and (b) are showing this for $\mathcal{A} = 0.5$ and $\mathcal{A} = 10.0$, respectively. For $\alpha_{a_H} = 0.2$, plots (c) and (d) are showing the same for $\mathcal{A} = 0.5$ and $\mathcal{A} = 10.0$, respectively.

Appendices

A Relation between the proper times of the detectors

The uniformly accelerated detectors follow hyperbolic paths on the Minkowski spacetime. These trajectories for different accelerations never meet each other except at null past ($t = -x$) and null future ($t = x$). Whereas the $(t/x) = \text{constant}$ lines are straight lines on the $x - t$ plane, passing through the origine, and one such line meets all hyperbola trajectories. Therefore all the accelerated frames will assign same value of (t/x) ($= C_0$, say) where a particular $(t/x) = C_0$ line meets all the corresponding trajectories. On the other hand the proper times of our present detectors are extended from $-\infty$ to $+\infty$ and so they starts simultaneously from the null past horizon ($t/x = -1$) and reach at future null horizon ($t/x = 1$) again simultaneously. Also if both the detectors starts from same $t/x = \text{constant}$ line, then at each moment they will measure the same t/x , but different from the initial value. This simple setup is very useful to find a relation between the individual proper times of the frames. Moreover usually the relation between proper times of two different frames are done by using a quantity which is “numerically” same for both the frames (like the infinitesimal spacetime distant element dS^2). The above discussion implies that a particular $t/x = \text{constant}$ (C_0 , say) line therefore can be used to connect the two hyperbolic trajectories, in particular to find the relation between the proper times of these frames. The same idea and simplest situation was adopted in [17] (see the start of the section 2 of this reference) as well. Here also we will

seek the relation by considering the same idea.

Two detectors A and B that are uniformly accelerating in the same Rindler wedge (namely RRW) with accelerations a_A and a_B , respectively. Their trajectories in terms of their proper times are determined by the relation between the Minkowski coordinates and accelerated frame proper time:

$$\begin{aligned} t_A &= \frac{1}{a_A} \sinh(a_A \tau_A); & x_A &= \frac{1}{a_A} \cosh(a_A \tau_A), \\ t_B &= \frac{1}{a_B} \sinh(a_B \tau_B); & x_B &= \frac{1}{a_B} \cosh(a_B \tau_B). \end{aligned} \quad (\text{A.1})$$

Now using the fact that t/x is same for both these frames yields a relation between the proper times of the detectors as

$$\tau_B = \alpha_a \tau_A. \quad (\text{A.2})$$

This yields the required relation between the proper times of the detectors as (21) with $\alpha = \alpha_a = (a_A/a_B)$.

For anti-parallelly accelerating detectors A and B , with accelerations a_A and $-a_B$, respectively, then their trajectories in terms of their proper times are given by

$$\begin{aligned} t_A &= \frac{1}{a_A} \sinh(a_A \tau_A); & x_A &= \frac{1}{a_A} \cosh(a_A \tau_A), \\ t_B &= \frac{1}{a_B} \sinh(a_B \tau_B); & x_B &= -\frac{1}{a_B} \cosh(a_B \tau_B). \end{aligned} \quad (\text{A.3})$$

For detectors to be described by constant t/x or η , we obtain the following relation between the detectors' proper times

$$\tau_B = -\alpha_a \tau_A. \quad (\text{A.4})$$

In this case, therefore we have $\tau_B = \alpha \tau_a$ where $\alpha = -\alpha_a = -(a_A/a_B)$.

If the detectors are moving with constant velocities and have relative velocity v_{rel} . Then we can have $\tau_B = \alpha_v \tau_A$, where

$$\alpha_v = \sqrt{1 - v_{rel}^2}. \quad (\text{A.5})$$

For the detectors are moving with same constant velocity, then $v_{rel} = 0$ and hence $\alpha_v = 1$.

B Calculation of the late time density matrix

In this Appendix, we will briefly calculate the change in the density matrix ($\delta\rho$) of two detectors in stage II or stage IV, where two detectors uniformly accelerate and interacts with the background massless real scalar quantum field through monopole coupling. This calculation is for both heating process (H) and cooling process (C). Therefore we drop the subscripts H or C , used in the main text and keep it as a general discussion. Also the energy gap of the combined system is taken as ω (instead of ω_1 or ω_2 used in the main text). This interaction is governed by the action given by

$$S_{int} = \int c_A \chi_A(\tau_A) m_A(\tau_A) \phi(\bar{x}_A) d\tau_A + \int c_B \chi_B(\tau_B) m_B(\tau_B) \phi(\bar{x}_B) d\tau_B. \quad (\text{B.1})$$

We choose the initial state of the combined system in the asymptotic past as

$$|in\rangle = |0\rangle|D\rangle = |0\rangle[b_1|e_A g_B\rangle + b_2|g_A e_B\rangle], \quad (\text{B.2})$$

where $|0\rangle$ is the vacuum of the quantum field in tensor product with the entangled state of the detectors. In the above we will choose $b_1 = (1/\sqrt{2}) = b_2$ for $|s\rangle$, $b_1 = (1/\sqrt{2})$, $b_2 = -(1/\sqrt{2})$ for $|a\rangle$ and $b_1 \neq 1/\sqrt{2}$ ($0 < b_1 < 1$), $b_2 = \pm\sqrt{1 - b_1^2}$ for non-maximally entangled states in the main analysis of our paper. At the asymptotic future, the evolved quantum state can be given by [30]

$$|out\rangle = T e^{iS_{int}} |in\rangle. \quad (\text{B.3})$$

Here T denotes the time order product of the operators.

The reduced density matrix of the detectors can be obtained by tracing out the field part of the final density matrix [29]

$$\rho_{AB} = \text{Tr}_\phi |out\rangle\langle out|. \quad (\text{B.4})$$

The elements of the reduced density matrix are evaluated from the Dyson series expansion of (B.3) upto second order in c_j inside (B.4):

$$\begin{aligned}
& \langle n_A n_B | \rho_{AB} | \hat{n}_A \hat{n}_B \rangle \\
&= \text{Tr}_\phi \langle n_A n_B | [1 + iS_{int} - T(S_{int} S'_{int}/2)] [b_1 |e_{AGB}\rangle + b_2 |g_A e_B\rangle] |0\rangle \langle 0 | [b_1^* \langle e_{AGB}| + b_2^* \langle g_A e_B|] \\
& \quad [1 - iS_{int} - T(S_{int} S'_{int}/2)] | \hat{n}_A \hat{n}_B \rangle \\
&= \langle n_A n_B | [b_1 |e_{AGB}\rangle + b_2 |g_A e_B\rangle] [b_1^* \langle e_{AGB}| + b_2^* \langle g_A e_B|] | \hat{n}_A \hat{n}_B \rangle \\
& \quad + \text{Tr}_\phi \langle n_A n_B | S_{int} |0\rangle [b_1 |e_{AGB}\rangle + b_2 |g_A e_B\rangle] [b_1^* \langle e_{AGB}| + b_2^* \langle g_A e_B|] \langle 0 | S_{int} | \hat{n}_A \hat{n}_B \rangle \\
& \quad - \text{Tr}_\phi \langle n_A n_B | T[S_{int} S'_{int}/2] |0\rangle \langle 0 | [b_1 |e_{AGB}\rangle + b_2 |g_A e_B\rangle] [b_1^* \langle e_{AGB}| + b_2^* \langle g_A e_B|] | \hat{n}_A \hat{n}_B \rangle \\
& \quad - \text{Tr}_\phi \langle n_A n_B | [b_1 |e_{AGB}\rangle + b_2 |g_A e_B\rangle] [b_1^* \langle e_{AGB}| + b_2^* \langle g_A e_B|] |0\rangle \langle 0 | T[S_{int} S'_{int}/2] | \hat{n}_A \hat{n}_B \rangle \\
&= \rho_0 + \underbrace{[R_{n_A n_B, \hat{n}_A \hat{n}_B}^{(1)} + R_{n_A n_B, \hat{n}_A \hat{n}_B}^{(2)} + R_{\hat{n}_A \hat{n}_B, n_A n_B}^{(2)*}]}_{O(c^2)}, \tag{B.5}
\end{aligned}$$

where ρ_0 is the initial density matrix in the bases of $|e_A e_B\rangle$, $|e_{AGB}\rangle$, $|g_A e_B\rangle$ and $|g_{AGB}\rangle$, given by

$$\rho_0 = \begin{pmatrix} 0 & 0 & 0 & 0 \\ 0 & |b_1|^2 & b_1 b_2^* & 0 \\ 0 & b_2 b_1^* & |b_2|^2 & 0 \\ 0 & 0 & 0 & 0 \end{pmatrix}. \tag{B.6}$$

Terms first order in c_j vanishes individually due to the trace operation ($\langle 0_M | \phi(\bar{x}_i) | 0_M \rangle = 0$) and the terms second order in c_j are calculated as follows:

$$\begin{aligned}
R_{n_A n_B, \hat{n}_A \hat{n}_B}^{(1)} &= \text{Tr}_\phi \langle n_A n_B | S_{int} [b_1 |e_{AGB}\rangle + b_2 |g_A e_B\rangle] |0\rangle \langle 0 | [b_1^* \langle e_{AGB}| + b_2^* \langle g_A e_B|] S_{int} | \hat{n}_A \hat{n}_B \rangle \\
&= \text{Tr}_\phi \langle n_A n_B | \left(\int c_A \chi_A(\tau_A) m_A(\tau_A) \phi(\bar{x}_A) d\tau_A + \int c_B \chi_B(\tau_B) m_B(\tau_B) \phi(\bar{x}_B) d\tau_B \right) \\
& \quad [b_1 |e_{AGB}\rangle + b_2 |g_A e_B\rangle] |0\rangle \langle 0 | [b_1^* \langle e_{AGB}| + b_2^* \langle g_A e_B|] \\
& \quad \left(\int c_A \chi_A(\tau_A) m_A(\tau_A) \phi(\bar{x}_A) d\tau_A + \int c_B \chi_B(\tau_B) m_B(\tau_B) \phi(\bar{x}_B) d\tau_B \right) | \hat{n}_A \hat{n}_B \rangle \\
&= \text{Tr}_\phi \left(\int d\tau_A c_A \chi_A(\tau_A) \langle n_A n_B | m_A(\tau_A) [b_1 |e_{AGB}\rangle + b_2 |g_A e_B\rangle] \phi(\bar{x}_A) |0\rangle \right. \\
& \quad \left. + \int d\tau_B c_B \chi_B(\tau_B) \langle n_A n_B | m_B(\tau_B) [b_1 |e_{AGB}\rangle + b_2 |g_A e_B\rangle] \phi(\bar{x}_B) |0\rangle \right) \\
& \quad \left(\int d\tau'_A c_A \chi_A(\tau'_A) [b_1^* \langle e_{AGB}| + b_2^* \langle g_A e_B|] m_A(\tau'_A) | \hat{n}_A \hat{n}_B \rangle \langle 0 | \phi(\bar{x}'_A) \right. \\
& \quad \left. + \int d\tau'_B c_B \chi_B(\tau'_B) [b_1^* \langle e_{AGB}| + b_2^* \langle g_A e_B|] m_B(\tau'_B) | \hat{n}_A \hat{n}_B \rangle \langle 0 | \phi(\bar{x}'_B) \right) \\
&= \text{Tr}_\phi \left[\int d\tau_A c_A \chi_A(\tau_A) [b_1 e^{i(g_A - e_A)\tau_A} \delta_{n_A, g_A} \delta_{n_B, g_B} + b_2 e^{i(e_A - g_A)\tau_A} \delta_{n_A, e_A} \delta_{n_B, e_B}] \phi(\bar{x}_A) |0\rangle \right. \\
& \quad \left. + \int d\tau_B c_B \chi_B(\tau_B) [b_1 e^{i(e_B - g_B)\tau_B} \delta_{n_A, e_A} \delta_{n_B, e_B} + b_2 e^{i(g_B - e_B)\tau_B} \delta_{n_A, g_A} \delta_{n_B, g_B}] \phi(\bar{x}_B) |0\rangle \right] \\
& \quad \left[\int d\tau'_A c_A \chi_A(\tau'_A) [b_1^* e^{i(e_A - g_A)\tau'_A} \delta_{\hat{n}_A, g_A} \delta_{\hat{n}_B, g_B} + b_2^* e^{i(g_A - e_A)\tau'_A} \delta_{\hat{n}_A, e_A} \delta_{\hat{n}_B, e_B}] \langle 0 | \bar{\phi}(\bar{x}'_A) \right. \\
& \quad \left. + \int d\tau'_B c_B \chi_B(\tau'_B) [b_1^* e^{i(g_B - e_B)\tau'_B} \delta_{\hat{n}_A, e_A} \delta_{\hat{n}_B, e_B} + b_2^* e^{i(e_B - g_B)\tau'_B} \delta_{\hat{n}_A, g_A} \delta_{\hat{n}_B, g_B}] \langle 0 | \bar{\phi}(\bar{x}'_B) \right] \\
&\equiv AA_{n_A n_B, \hat{n}_A \hat{n}_B} + AB_{n_A n_B, \hat{n}_A \hat{n}_B} + BB_{n_A n_B, \hat{n}_A \hat{n}_B} + BA_{n_A n_B, \hat{n}_A \hat{n}_B}, \tag{B.7}
\end{aligned}$$

where $e_j = \omega/2$ and $g_j = -\omega/2$, are the energy levels of the individual detectors. The positive frequency

Wightman function, $G^+(\tau_A, \tau_B)$ is obtained as

$$\begin{aligned}
G^+(\tau_A, \tau_B) &= \text{Tr}_\phi \left[\phi(\bar{x}_B) |0\rangle \langle 0| \phi(\bar{x}_A) \right] \\
&= \sum_{\text{all field states}(n)} \langle n | \phi(\bar{x}_B) |0\rangle \langle 0 | \phi(\bar{x}_A) |n\rangle \\
&= \langle 0 | \phi(\bar{x}_A) \left(\sum_n |n\rangle \langle n| \right) \phi(\bar{x}_B) |0\rangle \\
&= \langle 0 | \phi(\bar{x}_A) \phi(\bar{x}_B) |0\rangle
\end{aligned} \tag{B.8}$$

where *completeness* identity of the field states has been used in the last equality. We have

$$\begin{aligned}
AA &= \int \int c_A^2 \chi_A(\tau_A) \chi_A(\tau'_A) d\tau_A d\tau'_A G^+(\bar{x}'_A, \bar{x}_A) \begin{pmatrix} |b_2|^2 e^{i\omega(\tau_A - \tau'_A)} & 0 & 0 & b_2 b_1^* e^{i\omega(\tau_A + \tau'_A)} \\ 0 & 0 & 0 & 0 \\ 0 & 0 & 0 & 0 \\ b_1 b_2^* e^{i\omega(-\tau_A - \tau'_A)} & 0 & 0 & |b_1|^2 e^{i\omega(-\tau_A + \tau'_A)} \end{pmatrix} \\
&= \begin{pmatrix} |b_2|^2 \mathcal{P}_A(\omega) & 0 & 0 & b_2 b_1^* \mathcal{P}_{AA}(\omega) \\ 0 & 0 & 0 & 0 \\ 0 & 0 & 0 & 0 \\ b_1 b_2^* \mathcal{P}_{AA}(-\omega) & 0 & 0 & |b_1|^2 \mathcal{P}_A(-\omega) \end{pmatrix},
\end{aligned} \tag{B.9}$$

$$\begin{aligned}
BB &= \int \int c_B^2 \chi_B(\tau_B) \chi_B(\tau'_B) d\tau_B d\tau'_B G^+(\bar{x}'_B, \bar{x}_B) \begin{pmatrix} |b_1|^2 e^{i\omega(\tau_B - \tau'_B)} & 0 & 0 & b_1 b_2^* e^{i\omega(\tau_B + \tau'_B)} \\ 0 & 0 & 0 & 0 \\ 0 & 0 & 0 & 0 \\ b_2 b_1^* e^{i\omega(-\tau_B - \tau'_B)} & 0 & 0 & |b_2|^2 e^{i\omega(-\tau_B + \tau'_B)} \end{pmatrix} \\
&= \begin{pmatrix} |b_1|^2 \mathcal{P}_B(\omega) & 0 & 0 & b_1 b_2^* \mathcal{P}_{BB}(\omega) \\ 0 & 0 & 0 & 0 \\ 0 & 0 & 0 & 0 \\ b_2 b_1^* \mathcal{P}_{BB}(-\omega) & 0 & 0 & |b_2|^2 \mathcal{P}_B(-\omega) \end{pmatrix},
\end{aligned} \tag{B.10}$$

$$\begin{aligned}
AB &= \int \int c_A c_B \chi_A(\tau_A) \chi_B(\tau'_B) d\tau_A d\tau'_B G^+(\bar{x}'_B, \bar{x}_A) \begin{pmatrix} b_2 b_1^* e^{i\omega(\tau_A - \tau'_B)} & 0 & 0 & |b_2|^2 e^{i\omega(\tau_A + \tau'_B)} \\ 0 & 0 & 0 & 0 \\ 0 & 0 & 0 & 0 \\ |b_1|^2 e^{-i\omega(\tau_A + \tau'_B)} & 0 & 0 & b_1 b_2^* e^{-i\omega(\tau_A - \tau'_B)} \end{pmatrix} \\
&= \begin{pmatrix} b_2 b_1^* \mathcal{P}_{AB}(\omega, -\omega) & 0 & 0 & |b_2|^2 \mathcal{P}_{AB}(\omega, \omega) \\ 0 & 0 & 0 & 0 \\ 0 & 0 & 0 & 0 \\ |b_1|^2 \mathcal{P}_{AB}(-\omega, -\omega) & 0 & 0 & b_1 b_2^* \mathcal{P}_{AB}(-\omega, \omega) \end{pmatrix},
\end{aligned} \tag{B.11}$$

$$\begin{aligned}
BA &= \int \int c_A c_B \chi_A(\tau'_A) \chi_B(\tau_B) d\tau'_A d\tau_B G^+(\bar{x}'_A, \bar{x}_B) \begin{pmatrix} b_1 b_2^* e^{-i\omega(\tau'_A - \tau_B)} & 0 & 0 & |b_1|^2 e^{i\omega(\tau'_A + \tau_B)} \\ 0 & 0 & 0 & 0 \\ 0 & 0 & 0 & 0 \\ |b_2|^2 e^{-i\omega(\tau'_A + \tau_B)} & 0 & 0 & b_2 b_1^* e^{i\omega(\tau'_A - \tau_B)} \end{pmatrix} \\
&= \begin{pmatrix} b_1 b_2^* \mathcal{P}_{AB}^*(\omega, -\omega) & 0 & 0 & |b_1|^2 \mathcal{P}_{AB}^*(-\omega, -\omega) \\ 0 & 0 & 0 & 0 \\ 0 & 0 & 0 & 0 \\ |b_2|^2 \mathcal{P}_{AB}^*(\omega, \omega) & 0 & 0 & b_2 b_1^* \mathcal{P}_{AB}^*(-\omega, \omega) \end{pmatrix},
\end{aligned} \tag{B.12}$$

where $\mathcal{P}_j(\pm\omega)$ is defined by (15). We denote

$$\mathcal{P}_{jj}(\pm\omega) = c_j^2 \int \int \chi_j(\tau_j) \chi_j(\tau'_j) d\tau_j d\tau'_j G^+(\bar{x}'_j, \bar{x}_j) e^{\pm i\omega(\tau_j + \tau'_j)}, \tag{B.13}$$

$$\mathcal{P}_{AB}(\pm\omega, \pm\omega) = c_A c_B \int \int d\tau_A d\tau_B e^{i(\pm\omega\tau_A \pm \omega\tau_B)} G^+(\bar{x}'_B, \bar{x}_A). \tag{B.14}$$

Using these definitions, we can identify that the matrix BA as hermitian conjugate of matrix AB .

The positive frequency Wightman function $G^+(\bar{x}', \bar{x})$ can be written as $G^+(\tau', \tau)$, satisfies the following properties

$$G^+(-\tau_i, -\tau_j) = G^+(\tau_j, \tau_i); \quad G^+(\tau_i, \tau_j) = [G^+(\tau_j, \tau_i)]^*. \quad (\text{B.15})$$

Using the above properties of the positive frequency Wightman function, we can check that \mathcal{P}_{AB} (similarly, \mathcal{P}_j) is a real quantity, as

$$\begin{aligned} \mathcal{P}_{AB}(\pm\omega, \pm\omega) &= c_A c_B \int \int d\tau_A d\tau_B e^{i(\pm\omega\tau_A \pm \omega\tau_B')} G^+(\tau_B', \tau_A) \\ &= c_A c_B \int \int d\tau_A d\tau_B e^{-i(\pm\omega\tau_A \pm \omega\tau_B')} G^+(-\tau_B', -\tau_A) \\ &= c_A c_B \int \int d\tau_A d\tau_B e^{-i(\pm\omega\tau_A \pm \omega\tau_B')} [G^+(\tau_B', \tau_A)]^* \\ &= \mathcal{P}_{AB}^*(\pm\omega, \pm\omega), \end{aligned} \quad (\text{B.16})$$

where after the second equality, we have changed $\tau_j \rightarrow -\tau_j$. Then, we have used the property of the Wightman function, given in (B.15).

The final expression of $R^{(1)}$ can be obtained by adding (B.9), (B.10), (B.11) and (B.12), as

$$R^{(1)} = \begin{pmatrix} |b_2|^2 \mathcal{P}_A(\omega) + |b_1|^2 \mathcal{P}_B(\omega) & 0 & 0 & b_2 b_1^* \mathcal{P}_{AA}(\omega) + b_1 b_2^* \mathcal{P}_{BB}(\omega) \\ +b_2 b_1^* \mathcal{P}_{AB}(\omega, -\omega) + b_1 b_2^* \mathcal{P}_{AB}(\omega, -\omega) & & +|b_2|^2 \mathcal{P}_{AB}(\omega, \omega) + |b_1|^2 \mathcal{P}_{AB}(-\omega, -\omega) & \\ 0 & 0 & 0 & 0 \\ 0 & 0 & 0 & 0 \\ b_1 b_2^* \mathcal{P}_{AA}(-\omega) + b_2 b_1^* \mathcal{P}_{BB}(-\omega) & 0 & 0 & |b_1|^2 \mathcal{P}_A(-\omega) + |b_2|^2 \mathcal{P}_B(-\omega) \\ +|b_1|^2 \mathcal{P}_{AB}(-\omega, -\omega) + |b_2|^2 \mathcal{P}_{AB}(\omega, \omega) & & +b_1 b_2^* \mathcal{P}_{AB}(-\omega, \omega) + b_2 b_1^* \mathcal{P}_{AB}(-\omega, \omega) & \end{pmatrix}, \quad (\text{B.17})$$

where we have used the identity (B.16).

Next we calculate the following term:

$$\begin{aligned}
& R_{n_A n_B, \hat{n}_A \hat{n}_B}^{(2)} \\
&= -\text{Tr}_\phi \langle n_A n_B | T(S_{int} S'_{int}/2) | 0 \rangle \langle 0 | [b_1 |e_{AgB}\rangle + b_2 |g_A e_B\rangle] [b_1^* \langle e_{AgB}| + b_2^* \langle g_A e_B|] | \hat{n}_A \hat{n}_B \rangle \\
&= -\langle n_A n_B | \langle 0 | T \left[\left(\int d\tau_A c_A \chi_A(\tau_A) m_A(\tau_A) \phi(\bar{x}_A) + \int d\tau_B c_B \chi_B(\tau_B) m_B(\tau_B) \phi(\bar{x}_B) \right) \left(\int d\tau'_A c_A \chi_A(\tau'_A) \right. \right. \\
& \quad \left. \left. m_A(\tau'_A) \phi(\bar{x}'_A) + \int d\tau'_B c_B \chi_B(\tau'_B) m_B(\tau'_B) \phi(\bar{x}'_B) \right) / 2 \right] | 0 \rangle [b_1 |e_{AgB}\rangle + b_2 |g_A e_B\rangle] [b_1^* \langle e_{AgB}| + b_2^* \langle g_A e_B|] | \hat{n}_A \hat{n}_B \rangle \\
&= -\langle n_A n_B | \langle 0 | T \left[\left(c_A^2 \int \int d\tau_A d\tau'_A \chi_A(\tau_A) \chi_A(\tau'_A) m_A(\tau_A) m_A(\tau'_A) \phi(x_A) \phi(\bar{x}'_A) \right. \right. \\
& \quad \left. \left. + c_B^2 \int \int d\tau_B d\tau'_B \chi_B(\tau_B) \chi_B(\tau'_B) m_B(\tau_B) m_B(\tau'_B) \phi(x_B) \phi(\bar{x}'_B) + c_A c_B \int \int d\tau_B d\tau'_A \chi_B(\tau_B) \chi_A(\tau'_A) \right. \right. \\
& \quad \left. \left. m_B(\tau_B) m_A(\tau'_A) \phi(\bar{x}_B) \phi(\bar{x}'_A) + c_A c_B \int \int d\tau_A d\tau'_B m_A(\tau_A) m_B(\tau'_B) \chi_A(\tau_A) \chi_B(\tau'_B) \phi(\bar{x}_A) \phi(\bar{x}'_B) \right) / 2 \right] | 0 \rangle \\
& \quad [b_1 |e_{AgB}\rangle + b_2 |g_A e_B\rangle] [b_1^* \langle e_{AgB}| + b_2^* \langle g_A e_B|] | \hat{n}_A \hat{n}_B \rangle \\
& \quad [\text{Now assuming non-primed proper times are greater than primed proper times, i.e., } \tau > \tau', \text{ see[30]}] \\
&= -\langle n_A n_B | \left[\left(c_A^2 \int \int d\tau_A d\tau'_A \chi_A(\tau_A) \chi_A(\tau'_A) m_A(\tau_A) m_A(\tau'_A) \Theta(\tau_A - \tau'_A) G_W(\bar{x}_A, \bar{x}'_A) \right. \right. \\
& \quad \left. \left. + c_B^2 \int \int d\tau_B d\tau'_B \chi_B(\tau_B) \chi_B(\tau'_B) m_B(\tau_B) m_B(\tau'_B) \Theta(\tau_B - \tau'_B) G_W(\bar{x}_B, \bar{x}'_B) \right. \right. \\
& \quad \left. \left. + c_A c_B \int \int d\tau_B d\tau'_A \chi_B(\tau_B) \chi_A(\tau'_A) m_B(\tau_B) m_A(\tau'_A) \Theta(\tau_B - \tau'_A) G_W(\bar{x}_B, \bar{x}'_A) \right. \right. \\
& \quad \left. \left. + c_A c_B \int \int d\tau_A d\tau'_B \chi_A(\tau_A) \chi_B(\tau'_B) m_A(\tau_A) m_B(\tau'_B) \Theta(\tau_A - \tau'_B) G_W(\bar{x}_A, \bar{x}'_B) \right) \right] [b_1 |e_{AgB}\rangle + b_2 |g_A e_B\rangle] \\
& \quad [b_1^* \delta_{\hat{n}_A, e_A} \delta_{\hat{n}_B, g_B} + b_2^* \delta_{\hat{n}_A, g_A} \delta_{\hat{n}_B, e_B}] \\
&= -\langle n_A n_B | \left(c_A^2 \int \int d\tau_A d\tau'_A \chi_A(\tau_A) \chi_A(\tau'_A) m_A(\tau_A) m_A(\tau'_A) [b_1 |e_{AgB}\rangle + b_2 |g_A e_B\rangle] \Theta(\tau_A - \tau'_A) G_W(\bar{x}_A, \bar{x}'_A) \right. \\
& \quad \left. + c_B^2 \int \int d\tau_B d\tau'_B \chi_B(\tau_B) \chi_B(\tau'_B) m_B(\tau_B) m_B(\tau'_B) [b_1 |e_{AgB}\rangle + b_2 |g_A e_B\rangle] \Theta(\tau_B - \tau'_B) G_W(\bar{x}_B, \bar{x}'_B) \right. \\
& \quad \left. + c_A c_B \int \int d\tau_B d\tau'_A \chi_B(\tau_B) \chi_A(\tau'_A) m_B(\tau_B) m_A(\tau'_A) [b_1 |e_{AgB}\rangle + b_2 |g_A e_B\rangle] \Theta(\tau_B - \tau'_A) G_W(\bar{x}_B, \bar{x}'_A) \right. \\
& \quad \left. + c_A c_B \int \int d\tau_A d\tau'_B \chi_A(\tau_A) \chi_B(\tau'_B) m_A(\tau_A) m_B(\tau'_B) [b_1 |e_{AgB}\rangle + b_2 |g_A e_B\rangle] \Theta(\tau_A - \tau'_B) G_W(\bar{x}_A, \bar{x}'_B) \right) \\
& \quad [b_1^* \delta_{\hat{n}_A, e_A} \delta_{\hat{n}_B, g_B} + b_2^* \delta_{\hat{n}_A, g_A} \delta_{\hat{n}_B, e_B}] \\
&= -\left(c_A^2 \int \int d\tau_A d\tau'_A \chi_A(\tau_A) \chi_A(\tau'_A) [b_1 e^{i\omega\tau_A} e^{-i\omega\tau'_A} \delta_{n_A, e_A} \delta_{n_B, g_B} + b_2 e^{-i\omega\tau_A} e^{i\omega\tau'_A} \delta_{n_A, g_A} \delta_{n_B, e_B}] \Theta(\tau_A - \tau'_A) G_W(\bar{x}_A, \bar{x}'_A) \right. \\
& \quad \left. + c_B^2 \int \int d\tau_B d\tau'_B \chi_B(\tau_B) \chi_B(\tau'_B) [b_1 e^{-i\omega\tau_B} e^{i\omega\tau'_B} \delta_{n_A, e_A} \delta_{n_B, g_B} + b_2 e^{i\omega\tau_B} e^{-i\omega\tau'_B} \delta_{n_A, g_A} \delta_{n_B, e_B}] \Theta(\tau_B - \tau'_B) G_W(\bar{x}_B, \bar{x}'_B) \right. \\
& \quad \left. + c_A c_B \int \int d\tau_B d\tau'_A \chi_B(\tau_B) \chi_A(\tau'_A) [b_1 e^{i\omega\tau_B - i\omega\tau'_A} \delta_{n_A, g_A} \delta_{n_B, e_B} + b_2 e^{-i\omega\tau_B + i\omega\tau'_A} \delta_{n_A, e_A} \delta_{n_B, g_B}] \Theta(\tau_B - \tau'_A) G_W(\bar{x}_B, \bar{x}'_A) \right. \\
& \quad \left. + c_A c_B \int \int d\tau_A d\tau'_B \chi_A(\tau_A) \chi_B(\tau'_B) [b_1 e^{i\omega\tau'_B - i\omega\tau_A} \delta_{n_A, g_A} \delta_{n_B, e_B} + b_2 e^{-i\omega\tau'_B + i\omega\tau_A} \delta_{n_A, e_A} \delta_{n_B, g_B}] \Theta(\tau_A - \tau'_B) G_W(\bar{x}_A, \bar{x}'_B) \right) \\
& \quad [b_1^* \delta_{\hat{n}_A, e_A} \delta_{\hat{n}_B, g_B} + b_2^* \delta_{\hat{n}_A, g_A} \delta_{\hat{n}_B, e_B}] \\
&= -\left(c_A^2 \int \int d\tau_A d\tau'_A \chi_A(\tau_A) \chi_A(\tau'_A) [b_1 e^{i\omega(\tau_A - \tau'_A)} \delta_{n_A, e_A} \delta_{n_B, g_B} + b_2 e^{-i\omega(\tau_A - \tau'_A)} \delta_{n_A, g_A} \delta_{n_B, e_B}] \Theta(\tau_A - \tau'_A) G_W(\bar{x}_A, \bar{x}'_A) \right. \\
& \quad \left. + c_B^2 \int \int d\tau_B d\tau'_B \chi_B(\tau_B) \chi_B(\tau'_B) [b_1 e^{-i\omega(\tau_B - \tau'_B)} \delta_{n_A, e_A} \delta_{n_B, g_B} + b_2 e^{i\omega(\tau_B - \tau'_B)} \delta_{n_A, g_A} \delta_{n_B, e_B}] \Theta(\tau_B - \tau'_B) G_W(\bar{x}_B, \bar{x}'_B) \right. \\
& \quad \left. + c_A c_B \int \int d\tau_A d\tau'_B \chi_A(\tau_A) \chi_B(\tau'_B) [b_1 e^{-i\omega(\tau_A - \tau'_B)} \delta_{n_A, g_A} \delta_{n_B, e_B} + b_2 e^{i\omega(\tau_A - \tau'_B)} \delta_{n_A, e_A} \delta_{n_B, g_B}] [iG_F(\bar{x}_A, \bar{x}'_B)] \right) \\
& \quad [b_1^* \delta_{\hat{n}_A, e_A} \delta_{\hat{n}_B, g_B} + b_2^* \delta_{\hat{n}_A, g_A} \delta_{\hat{n}_B, e_B}], \tag{B.18}
\end{aligned}$$

where in the third term after the second last equality, we have changed $\tau'_A \rightarrow \tau_A$ and $\tau_B \rightarrow \tau'_B$. Then we

used $\Theta(\tau_A - \tau'_B) + \Theta(\tau'_B - \tau_A) = 1$, to obtain the final expression.

This $R^{(2)}$ can be written in a matrix form, given by

$$R^{(2)} = - \begin{pmatrix} 0 & 0 & 0 & 0 \\ 0 & b_1^*(b_1 F_A(\omega) + b_1 F_B(-\omega) + b_2 \mathcal{E}(\omega)) & b_2^*(b_1 F_A(\omega) + b_1 F_B(-\omega) + b_2 \mathcal{E}(\omega)) & 0 \\ 0 & b_1^*(b_2 F_A(-\omega) + b_2 F_B(\omega) + b_1 \mathcal{E}(-\omega)) & b_2^*(b_2 F_A(-\omega) + b_2 F_B(\omega) + b_1 \mathcal{E}(-\omega)) & 0 \\ 0 & 0 & 0 & 0 \end{pmatrix}, \quad (\text{B.19})$$

where we defined

$$F_j(\pm\omega) = c_j^2 \int \int d\tau_j d\tau'_j \chi_j(\tau_j) \chi_j(\tau'_j) e^{\pm i\omega(\tau_j - \tau'_j)} \Theta(\tau_j - \tau'_j) G^+(\tau_j, \tau'_j), \quad (\text{B.20})$$

$$\mathcal{E}(\pm\omega) = c_A c_B \int \int d\tau_A d\tau'_B \chi_A(\tau_A) \chi_B(\tau'_B) e^{\pm i\omega(\tau_A - \tau'_B)} [iG_F(\tau_A, \tau'_B)]. \quad (\text{B.21})$$

One can see that $F_j(\pm\omega)$ satisfies the following relations,

$$\begin{aligned} & F_j(\pm\omega) + F_j^*(\pm\omega) \\ &= c_j^2 \int \int d\tau_j d\tau'_j \chi_j(\tau_j) \chi_j(\tau'_j) \left[e^{\pm i\omega(\tau_j - \tau'_j)} \Theta(\tau_j - \tau'_j) G^+(\tau_j, \tau'_j) + e^{\mp i\omega(\tau_j - \tau'_j)} \Theta(\tau_j - \tau'_j) G^+(\tau'_j, \tau_j) \right] \\ &= c_j^2 \int \int d\tau_j d\tau'_j \chi_j(\tau_j) \chi_j(\tau'_j) e^{\mp i\omega(\tau_j - \tau'_j)} G^+(\tau'_j, \tau_j) \\ &= \mathcal{P}_j(\mp\omega), \end{aligned} \quad (\text{B.22})$$

where in the first term of the second line we interchanged τ_j and τ'_j . Also, one finds

$$\begin{aligned} & F_j(\pm\omega) + F_j^*(\mp\omega) \\ &= c_j^2 \int \int d\tau_j d\tau'_j \chi_j(\tau_j) \chi_j(\tau'_j) \left[e^{\pm i\omega(\tau_j - \tau'_j)} \Theta(\tau_j - \tau'_j) G^+(\tau_j, \tau'_j) + e^{\pm i\omega(\tau_j - \tau'_j)} \Theta(\tau_j - \tau'_j) G^+(\tau'_j, \tau_j) \right] \\ &= c_j^2 \int \int d\tau_j d\tau'_j \chi_j(\tau_j) \chi_j(\tau'_j) e^{\pm i\omega(\tau_j - \tau'_j)} \Theta(\tau_j - \tau'_j) (G^+(\tau_j, \tau'_j) + G^+(\tau'_j, \tau_j)) \\ &\equiv Q_j(\pm\omega) = Q_j^*(\mp\omega). \end{aligned} \quad (\text{B.23})$$

$\mathcal{E}(\omega)$ satisfies the following relation

$$\begin{aligned} & \mathcal{E}(\omega) + \mathcal{E}^*(\omega) \\ &= c_A c_B \int \int d\tau_A d\tau'_B \chi_A(\tau_A) \chi_B(\tau'_B) e^{i\omega(\tau_A - \tau'_B)} [\Theta(\tau_A - \tau'_B) G^+(\tau_A, \tau'_B) + \Theta(\tau'_B - \tau_A) G^+(\tau'_B, \tau_A)] \\ &+ c_A c_B \int \int d\tau_A d\tau'_B \chi_A(\tau_A) \chi_B(\tau'_B) e^{-i\omega(\tau'_B - \tau_A)} [\Theta(\tau'_B - \tau_A) G^+(\tau_A, \tau'_B) + \Theta(\tau_A - \tau'_B) G^+(\tau'_B, \tau_A)] \\ &= c_A c_B \int \int d\tau_A d\tau'_B \chi_A(\tau_A) \chi_B(\tau'_B) e^{i\omega(\tau_A - \tau'_B)} [G^+(\tau_A, \tau'_B) + G^+(\tau'_B, \tau_A)] \\ &= \mathcal{P}_{AB}^*(-\omega, \omega) + \mathcal{P}_{AB}(\omega, -\omega) \\ &= \mathcal{P}_{AB}(-\omega, \omega) + \mathcal{P}_{AB}(\omega, -\omega), \end{aligned} \quad (\text{B.24})$$

where we interchanged τ_A and τ'_B in the second line. To arrive in the last equality, we have used the fact that \mathcal{P}_{AB} is a real quantity, see (B.16). Now adding (B.19) with it's hermitian conjugate, and using (B.22), (B.23) and (B.24), we obtain

$$R^{(2)} + R^{(2)\dagger} = - \begin{pmatrix} 0 & 0 & 0 & 0 \\ 0 & b_1^2(\mathcal{P}_A(-\omega) + \mathcal{P}_B(\omega)) + b_1 b_2(\mathcal{P}_{AB}(-\omega, \omega) + \mathcal{P}_{AB}(\omega, -\omega)) & b_1 b_2(Q_A(\omega) + Q_B(-\omega)) + b_2^2 \mathcal{E}(\omega) + b_1^2 \mathcal{E}^*(-\omega) & 0 \\ 0 & b_1 b_2(Q_A^*(\omega) + Q_B^*(-\omega)) + b_2^2 \mathcal{E}^*(\omega) + b_1^2 \mathcal{E}(-\omega) & b_2^2(\mathcal{P}_A(\omega) + \mathcal{P}_B(-\omega)) + b_1 b_2(\mathcal{P}_{AB}(-\omega, \omega) + \mathcal{P}_{AB}(\omega, -\omega)) & 0 \\ 0 & 0 & 0 & 0 \end{pmatrix}. \quad (\text{B.25})$$

Finally, by adding (B.17) and (B.25), we obtain the variation of the density matrix ($\delta\rho$) upto second order in c_i , as

$$\delta\rho = R^{(1)} + R^{(2)} + R^{(2)\dagger}. \quad (\text{B.26})$$

C Calculation of $\text{Tr}(\delta\rho^H h_{\alpha_k})$

To evaluate the trace (14), we need to add the diagonal terms of $\delta\rho^H h_{\alpha_k}$ ($k = v, \alpha_{a_H}, \alpha_{a_C}$). This is given by multiplication of matrices given by (B.26) and (10). We consider the coefficients of the initial detector state, b_1, b_2 are to be real numbers, satisfying $|b_1|^2 + |b_2|^2 = 1$. The diagonal terms are:

$$(\delta\rho^H h_{\alpha_k})_{e_A e_B, e_A e_B} = [b_2^2 \mathcal{P}_A(\omega) + b_1^2 \mathcal{P}_B(\omega) + 2b_1 b_2 \mathcal{P}_{AB}(\omega, -\omega)] \frac{1 + \alpha_k}{2}; \quad (\text{C.1})$$

$$(\delta\rho^H h_{\alpha_k})_{e_A g_B, e_A g_B} = -[b_1^2 (\mathcal{P}_A(-\omega) + \mathcal{P}_B(\omega)) + b_1 b_2 (\mathcal{P}_{AB}(\omega, -\omega) + \mathcal{P}_{AB}(-\omega, \omega))] \frac{1 - \alpha_k}{2}; \quad (\text{C.2})$$

$$(\delta\rho^H h_{\alpha_k})_{g_A e_B, g_A e_B} = -[b_2^2 (\mathcal{P}_A(\omega) + \mathcal{P}_B(-\omega)) + b_1 b_2 (\mathcal{P}_{AB}(\omega, -\omega) + \mathcal{P}_{AB}(-\omega, \omega))] \frac{-1 + \alpha_k}{2}; \quad (\text{C.3})$$

$$(\delta\rho^H h_{\alpha_k})_{g_A g_B, g_A g_B} = [b_1^2 \mathcal{P}_A(-\omega) + b_2^2 \mathcal{P}_B(-\omega) + 2b_1 b_2 \mathcal{P}_{AB}(-\omega, \omega)] \frac{-1 - \alpha_k}{2}. \quad (\text{C.4})$$

Trace of $\delta\rho^H h_{\alpha_k}$ is obtained as,

$$\begin{aligned} \text{Tr}[\delta\rho^H h_{\alpha_k}] &= \{b_2^2 \mathcal{P}_A(\omega) - b_1^2 \mathcal{P}_A(-\omega) + b_1 b_2 [\mathcal{P}_{AB}(\omega, -\omega) - \mathcal{P}_{AB}(-\omega, \omega)]\} \\ &\quad + \alpha_k \{b_1^2 \mathcal{P}_B(\omega) - b_2^2 \mathcal{P}_B(-\omega) + b_1 b_2 [\mathcal{P}_{AB}(\omega, -\omega) - \mathcal{P}_{AB}(-\omega, \omega)]\}. \end{aligned} \quad (\text{C.5})$$

This leads to (14) for any general initially entangled states.

D Calculation of $\mathcal{P}_j(\pm\omega)$

The expression of \mathcal{P}_j ($j = A, B$) is given by (15). The integrations need to be evaluated for qualitative analysis of efficiency of the cycle. As the interactions are turned on at time $-\mathcal{T}_j/2$ and runs upto time $\mathcal{T}_j/2$, the integration limits should be $-\mathcal{T}_j/2$ to $\mathcal{T}_j/2$. These integrations can not be done analytically due to their finite integration limits. However, we can extend the integration limits to $\pm\infty$ by choosing a suitable switching function. We choose the switching function given by (20), which is non-vanishing for $-\mathcal{T}_j/2 < \tau_j < \mathcal{T}_j/2$ and approximately vanishing outside this domain. $\mathcal{P}_j(\omega)$ can be expressed by (taking $c_A = c_B = 1$)

$$\mathcal{P}_j(\omega) = \int_{-\infty}^{\infty} \int_{-\infty}^{\infty} d\tau_j d\tau'_j \chi_j(\tau_j) \chi_j(\tau'_j) e^{i\omega(\tau_j - \tau'_j)} G^+(\tau'_j, \tau_j), \quad (\text{D.1})$$

To evaluate this quantity, we choose a coordinate transform

$$T = \tau_A + \tau'_A; \quad \sigma = \tau_A - \tau'_A. \quad (\text{D.2})$$

The Jacobian of this transformation is 1/2. In the case of evaluating \mathcal{P}_B , we use (A.2) while detector B is accelerating in RRW and (A.4) while in LRW to express the integrations in terms of τ_A and τ'_A . Use of (A.2) and (A.4) implies that

$$\begin{aligned} \chi_B(\tau_B) \chi_B(\tau'_B) &= \frac{(\mathcal{T}_B/2)^2}{\tau_B^2 + (\mathcal{T}_B/2)^2} \frac{(\mathcal{T}_B/2)^2}{\tau_B'^2 + (\mathcal{T}_B/2)^2} = \frac{(\pm\alpha_a \mathcal{T}_A/2)^2}{(\pm\alpha_a \tau_A)^2 + (\pm\alpha_a \mathcal{T}_A/2)^2} \frac{(\pm\alpha_a \mathcal{T}_A/2)^2}{(\pm\alpha_a \tau'_A)^2 + (\pm\alpha_a \mathcal{T}_A/2)^2} \\ &= \chi_A(\tau_A) \chi_A(\tau'_A) \end{aligned} \quad (\text{D.3})$$

With use of (D.2), we can express the combination of the switching functions as

$$\begin{aligned} \chi_j(\tau_j) \chi_j(\tau'_j) &= \frac{(\mathcal{T}_A/2)^2}{\tau_A^2 + (\mathcal{T}_A/2)^2} \frac{(\mathcal{T}_A/2)^2}{\tau_A'^2 + (\mathcal{T}_A/2)^2} \\ &= \frac{\mathcal{T}_A^4}{(T^2 - T_1^2)(T^2 - T_2^2)}, \end{aligned} \quad (\text{D.4})$$

where, $T_1 = \sigma + i\mathcal{T}_A$ and $T_2 = -\sigma + i\mathcal{T}_A$. The Wightman function in (D.1) for detector A can be written as a function of σ , as $G^+(\tau'_A, \tau_A) = [G^+(\tau_A, \tau'_A)]^* = [G^+(\sigma)]^*$. Then we can write (D.1) for $j = A$, as

$$\mathcal{P}_A(\pm\omega) = \frac{1}{2} \int_{-\infty}^{\infty} d\sigma e^{\pm i\omega\sigma} [G^+(\sigma)]^* \int_{-\infty}^{\infty} dT \frac{\mathcal{T}_A^4}{(T^2 - T_1^2)(T^2 - T_2^2)}, \quad (\text{D.5})$$

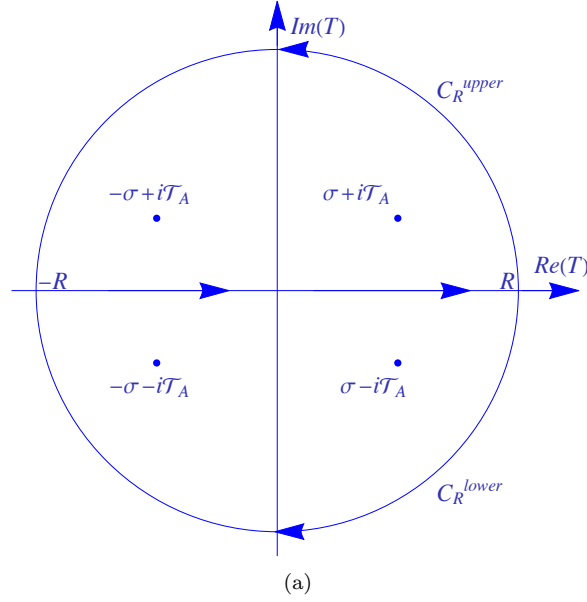


Figure 11: Plots showing contours of integral T . For an integrand like $f(T) = e^{\pm ikT}/[(T^2 - T_1^2)(T^2 - T_2^2)]$, we choose upper and lower contours for positive and negative sign of the exponential, respectively. For $k = 0$, we are free to choose any contour. Both will give same results.

To evaluate T -integral, we used the upper contour given in (fig:11) (see, [12, 13]). As an integrand like $f(T) = 1/[(T^2 - T_1^2)(T^2 - T_2^2)]$ vanishes for both $T \rightarrow \pm\infty$ ($\pm i\infty$), we are free to choose upper or lower contour. In upper contour, the poles are at $T = T_1$ and $T = T_2$. The integration results,

$$\begin{aligned}
\int_{-\infty}^{\infty} \frac{dT}{(T^2 - T_1^2)(T^2 - T_2^2)} &= 2\pi i \left(\text{Res}(f(T)) \Big|_{T=T_1} + \text{Res}(f(T)) \Big|_{T=T_2} \right) \\
&= 2\pi i \left(\frac{1}{2T_1(T_1^2 - T_2^2)} + \frac{1}{2T_2(T_2^2 - T_1^2)} \right) \\
&= \frac{\pi}{2\mathcal{T}_A(\sigma^2 + \mathcal{T}_A^2)}. \tag{D.6}
\end{aligned}$$

Therefore, (D.5) becomes

$$\mathcal{P}_A(\pm\omega) = \frac{\pi\mathcal{T}_A^3}{4} \int_{-\infty}^{\infty} \frac{d\sigma e^{\pm i\omega\sigma} [G^+(\sigma)]^*}{\sigma^2 + \mathcal{T}_A^2}, \tag{D.7}$$

- The positive frequency Wightman in Minkowski spacetime is given by [26]

$$G^+(\bar{x}, \bar{x}') = -\frac{1}{4\pi^2[(t - t' - i\epsilon)^2 - |x - x'|^2]}. \tag{D.8}$$

The trajectory of a uniformly accelerating observer moving in RRW and LRW is given in (18) and (19). One finds

$$\begin{aligned}
(t_j - t'_j - i\epsilon)^2 - |x_j - x'_j|^2 &= \left(\frac{1}{a_j} \sinh(a_j\tau_j) - \frac{1}{a_j} \sinh(a_j\tau'_j) - i\epsilon \right)^2 - \left| \pm \frac{1}{a_j} \cosh(a_j\tau_j) \mp \frac{1}{a_j} \cosh(a_j\tau'_j) \right|^2 \\
&= -\frac{2}{a_j^2} + \frac{2}{a_j^2} \left(\cosh(a_j\tau_j) \cosh(a_j\tau'_j) - \sinh(a_j\tau_j) \sinh(a_j\tau'_j) \right) - i\epsilon \\
&= -\frac{2}{a_j^2} (1 - [\cosh(a_j(\tau_j - \tau'_j)) - i\epsilon]) \\
&= -\frac{2}{a_j^2} (1 - \cosh(a_j(\tau_j - \tau'_j) - i\epsilon)) \\
&= \frac{4}{a_j^2} \sinh^2 \left(\frac{a_j(\tau_j - \tau'_j)}{2} - i\epsilon \right). \tag{D.9}
\end{aligned}$$

Therefore the positive frequency Wightman function of a uniformly accelerating detector is given by (see also in [26])

$$G^+(\tau_j, \tau'_j) = -\frac{a_j^2}{16\pi^2 \sinh^2(a_j(\tau_j - \tau'_j)/2 - i\epsilon)} = -\frac{1}{4\pi^2} \sum_{n=-\infty}^{\infty} \frac{1}{((\tau_j - \tau'_j) - i\epsilon - 2\pi in/a_j)^2}. \quad (\text{D.10})$$

where we have used $\frac{(a/2)^2}{\sinh^2(ax/2)} = \sum_{n=-\infty}^{\infty} \frac{1}{(x - i2\pi n/a)^2}$. Now using (D.10) for $j = A$ with (D.2), we can write (D.7) as

$$\mathcal{P}_A(\pm\omega) = -\frac{\mathcal{T}_A^3}{16\pi} \int_{-\infty}^{\infty} \frac{d\sigma e^{\pm i\omega\sigma}}{(\sigma^2 + \mathcal{T}_A^2)} \sum_{n=-\infty}^{\infty} \frac{1}{(\sigma + i\epsilon - 2\pi in/a_A)^2}. \quad (\text{D.11})$$

The summation in this expression can be split into three parts as

$$\begin{aligned} \mathcal{P}_A(\pm\omega) &= -\frac{\mathcal{T}_A^3}{16\pi} \int_{-\infty}^{\infty} \frac{d\sigma e^{\pm i\omega\sigma}}{\sigma^2 + \mathcal{T}_A^2} \left(\frac{1}{(\sigma + i\epsilon)^2} + \sum_{n=1}^{\infty} \frac{1}{\left(\sigma - \frac{i2\pi n}{a_A}\right)^2} + \sum_{n=1}^{\infty} \frac{1}{\left(\sigma + \frac{i2\pi n}{a_A}\right)^2} \right) \\ &= \mathcal{P}_{A,0}(\pm\omega) + \mathcal{P}_{A,n}(\pm\omega) + \mathcal{P}_{A,-n}(\pm\omega). \end{aligned} \quad (\text{D.12})$$

Poles contributing to $\mathcal{P}_A(\omega)$ are at $i\mathcal{T}_A$, $\frac{2\pi in}{a_A}$ and poles contributing to $\mathcal{P}_A(-\omega)$ are at $-i\epsilon$, $-i\mathcal{T}_A$, $-\frac{2\pi in}{a_A}$. The corresponding residues with factor $\pm 2\pi i$ are ($\epsilon \rightarrow 0$)

$$\begin{aligned} (2\pi i) \text{Res}(\mathcal{P}_A^{(I)}(\omega)) \Big|_{\sigma=i\mathcal{T}_A} &= \frac{\mathcal{T}_A^2 e^{-\mathcal{T}_A\omega}}{16} \left(\frac{1}{\mathcal{T}_A^2} + \sum_{n=1}^{\infty} \frac{1}{(\mathcal{T}_A - 2\pi n/a_A)^2} + \sum_{n=1}^{\infty} \frac{1}{(\mathcal{T}_A + 2\pi n/a_A)^2} \right) \\ &= \frac{(a_A \mathcal{T}_A/2)^2 e^{-\mathcal{T}_A\omega}}{16 \sin^2(a_A \mathcal{T}_A/2)}, \quad \left[\text{using, } \frac{(a/2)^2}{\sin^2(ax/2)} = \sum_{n=-\infty}^{\infty} \frac{1}{(x - 2\pi n/a)^2} \right] \\ &= (-2\pi i) \text{Res}(\mathcal{P}_A^{(I)}(-\omega)) \Big|_{\sigma=-i\mathcal{T}_A}, \end{aligned} \quad (\text{D.13})$$

$$\begin{aligned} (2\pi i) \sum_{n=1}^{\infty} \text{Res}(\mathcal{P}_{A,n}^{(I)}(\omega)) \Big|_{\sigma=\frac{2\pi in}{a_A}} &= \sum_{n=1}^{\infty} \frac{\mathcal{T}_A^3 e^{-\frac{2\pi n\omega}{a_A}} \left([\mathcal{T}_A^2 - \frac{4\pi^2 n^2}{a_A^2}] \omega - \frac{4\pi n}{a_A} \right)}{8 \left(\mathcal{T}_A^2 - \frac{4\pi^2 n^2}{a_A^2} \right)^2} \\ &= (-2\pi i) \sum_{n=1}^{\infty} \text{Res}(\mathcal{P}_{A,-n}^{(I)}(-\omega)) \Big|_{\sigma=-\frac{2\pi in}{a_A}}, \end{aligned} \quad (\text{D.14})$$

where

$$\begin{aligned} \sum_{n=1}^{\infty} \frac{\mathcal{T}_A^3 e^{-\frac{2\pi n\omega}{a_A}} \left([\mathcal{T}_A^2 - \frac{4\pi^2 n^2}{a_A^2}] \omega - \frac{4\pi n}{a_A} \right)}{8 \left(\mathcal{T}_A^2 - \frac{4\pi^2 n^2}{a_A^2} \right)^2} &= \frac{a_A^2 \mathcal{T}_A^2 e^{-\frac{2\pi\omega}{a_A}}}{64\pi^2} \left(\Phi \left(e^{-\frac{2\pi\omega}{a_A}}, 2, 1 + \frac{a_A \mathcal{T}_A}{2\pi} \right) - \Phi \left(e^{-\frac{2\pi\omega}{a_A}}, 2, 1 - \frac{a_A \mathcal{T}_A}{2\pi} \right) \right) \\ &\quad + \frac{a_A \mathcal{T}_A^2 \omega e^{-\frac{2\pi\omega}{a_A}}}{32\pi} \left(\Phi \left(e^{-\frac{2\pi\omega}{a_A}}, 1, 1 + \frac{a_A \mathcal{T}_A}{2\pi} \right) - \Phi \left(e^{-\frac{2\pi\omega}{a_A}}, 1, 1 - \frac{a_A \mathcal{T}_A}{2\pi} \right) \right) \end{aligned} \quad (\text{D.15})$$

and

$$(-2\pi i) \text{Res}(\mathcal{P}_{A,0}^{(I)}(-\omega)) \Big|_{\omega=-i\epsilon} = \frac{\mathcal{T}_A \omega}{8}. \quad (\text{D.16})$$

Here the notation, $\mathcal{P}_A^{(I)}$ means the integrand of the the quantity \mathcal{P}_A . Same notation also will be used in the following calculations. Using (D.15) and adding (D.13) and (D.14), we obtain expression of $\mathcal{P}_A(\omega)$, given in (22). Similarly, adding (D.13), (D.14) and (D.16), we obtain the expression of $\mathcal{P}_A(-\omega)$, given in (23).

\mathcal{P}_B in RRW: Using (A.2), (D.3) and (D.1), we can write \mathcal{P}_B as

$$\mathcal{P}_B(\pm\omega) = \alpha_a^2 \int_{-\infty}^{\infty} \int_{-\infty}^{\infty} d\tau_A d\tau'_A \chi_A(\tau_A) \chi_A(\tau'_A) e^{\pm i\omega \alpha_a (\tau_A - \tau'_A)} G_B^+(\alpha_a \tau'_A, \alpha_a \tau_A). \quad (\text{D.17})$$

The Wightman function for detector B can be written as (from (D.10))

$$\begin{aligned}
G_B^+(\alpha_a \tau_A, \alpha_a \tau'_A) &= G^+(\tau_B, \tau'_B) = -\frac{a_B^2}{16\pi^2 \sinh^2(a_B(\tau_B - \tau'_B)/2 - i\epsilon)} \\
&= -\frac{(a_A/\alpha_a)^2}{16\pi^2 \sinh^2(a_A(\tau_A - \tau'_A)/2 - i\epsilon)} \\
&= -\frac{1}{4\pi^2 \alpha_a^2} \sum_{n=-\infty}^{\infty} \frac{1}{(\sigma - i\epsilon - 2\pi i n/a_A)^2} .
\end{aligned} \tag{D.18}$$

Using the coordinate transformation given in (D.2) with (D.4), (D.6) and (D.18), we can write (D.17) as

$$\begin{aligned}
\mathcal{P}_B(\pm\omega) &= -\frac{\mathcal{T}_A^4}{8\pi^2} \int_{-\infty}^{\infty} \int_{-\infty}^{\infty} \frac{d\sigma dT e^{\pm i\omega \alpha_a \sigma}}{(T^2 - T_1^2)(T^2 - T_2^2)} \sum_{n=-\infty}^{\infty} \frac{1}{(\sigma + i\epsilon - \frac{2\pi i n}{a_A})^2} \\
&= -\frac{\mathcal{T}_A^3}{16\pi} \int_{-\infty}^{\infty} \frac{d\sigma e^{\pm i\omega \alpha_a \sigma}}{\sigma^2 + \mathcal{T}_A^2} \sum_{n=-\infty}^{\infty} \frac{1}{(\sigma + i\epsilon - \frac{2\pi i n}{a_A})^2} \\
&= \mathcal{P}_A(\pm\omega \alpha_a) .
\end{aligned} \tag{D.19}$$

The last equality comes from comparing expression of $\mathcal{P}_B(\pm\omega)$ after the second equality with expression of $\mathcal{P}_A(\pm\omega)$, given in (D.11). The only difference is presence of α_a with ω in (D.19). Therefore adding (D.13) and (D.14) with replacing ω with $\omega \alpha_a$ and using $\alpha_a = a_A/a_B$, gives expression of $\mathcal{P}_B(\omega)$ in (24). Similarly, adding (D.13), (D.14) and (D.16) with replacing ω with $\omega \alpha_a$ and using $\alpha_a = a_A/a_B$, gives expression of $\mathcal{P}_B(-\omega)$ in (25).

\mathcal{P}_B in LRW: Using (A.4), (D.3) and (D.1), we can write \mathcal{P}_B as

$$\begin{aligned}
\mathcal{P}_B(\pm\omega) &= \int_{-\infty}^{\infty} \int_{-\infty}^{\infty} d\tau_B d\tau'_B \chi_B(\tau_B) \chi_B(\tau'_B) e^{\pm i\omega(\tau_B - \tau'_B)} G^+(\tau'_B, \tau_B) \\
&= \alpha_a^2 \int_{-\infty}^{\infty} \int_{-\infty}^{\infty} d\tau_A d\tau'_A \chi_A(\tau_A) \chi_A(\tau'_A) e^{\mp i\omega \alpha_a(\tau_A - \tau'_A)} G^+(-\alpha_a \tau'_A, -\alpha_a \tau_A) \\
&= \alpha_a^2 \int_{-\infty}^{\infty} \int_{-\infty}^{\infty} d\tau_A d\tau'_A \chi_A(\tau_A) \chi_A(\tau'_A) e^{\pm i\omega \alpha_a(\tau_A - \tau'_A)} G^+(\alpha_a \tau'_A, \alpha_a \tau_A) ,
\end{aligned} \tag{D.20}$$

where in the last equality, we changed $\tau \rightarrow -\tau$ and we know that $G^+(\alpha_a \tau'_A, \alpha_a \tau_A) = [G^+(\alpha_a \tau_A, \alpha_a \tau'_A)]^*$. This expression of \mathcal{P}_B is same as given in (D.17). Thus

$$\mathcal{P}_B^{(LRW)}(\pm\omega) = \mathcal{P}_B^{(RRW)}(\pm\omega) = \mathcal{P}_B(\pm\omega) . \tag{D.21}$$

E Calculation of $\mathcal{P}_{AB}(\omega, -\omega) - \mathcal{P}_{AB}(-\omega, \omega)$

Using (A.2), (A.4) and (D.4), we obtain the combination of the switching functions for both detectors, as

$$\chi_A(\tau_A) \chi_B(\tau'_B) = \chi_A(\tau_A) \chi_A(\tau'_A) = \frac{\mathcal{T}_A^4}{(T^2 - T_1^2)(T^2 - T_2^2)} . \tag{E.1}$$

E.1 Acceleration in Same Direction

Using the coordinate transformation (D.2) with (A.2), we can write

$$\omega(\tau_A - \tau'_B) = \frac{\omega}{2}(\sigma + T - \alpha_a T + \alpha_a \sigma) = \frac{\omega T}{2}(1 - \alpha_a) + \frac{\omega \sigma}{2}(1 + \alpha_a) . \tag{E.2}$$

Using the trajectories given in (A.1), denominator of the green function can be evaluated as

$$\begin{aligned}
& (t_A - t'_B - i\epsilon)^2 - |x_A - x_B|^2 \\
&= \left(\frac{1}{a_A} \sinh(a_A \tau_A) - \frac{1}{a_B} \sinh(a_B \tau'_B) - i\epsilon \right)^2 - \left(\frac{1}{a_A} \cosh(a_A \tau_A) - \frac{1}{a_B} \cosh(a_B \tau'_B) \right)^2 \\
&= -\frac{1}{a_A^2} - \frac{1}{a_B^2} + \frac{2}{a_A a_B} (\cosh(a_A \tau_A) \cosh(a_B \tau'_B) - \sinh(a_A \tau_A) \sinh(a_B \tau'_B)) - i\epsilon \\
&= -\frac{2}{a_A a_B} \frac{1}{2} \left(\frac{a_A}{a_B} + \frac{a_B}{a_A} \right) + \frac{2}{a_A a_B} \cosh(a_A \sigma - i\epsilon) \\
&= \frac{2}{a_A a_B} [\cosh(a_A \sigma - i\epsilon) - \cosh(a_A \kappa)] \\
&= \frac{4}{a_A a_B} \sinh \left(\frac{a_A(\sigma - i\epsilon - \kappa)}{2} \right) \sinh \left(\frac{a_A(\sigma - i\epsilon + \kappa)}{2} \right), \tag{E.3}
\end{aligned}$$

here in the third equality, we used (A.2) and (D.2), and in the fourth equality we defined

$$\cosh(a_A \kappa) = \frac{1}{2} \left(\frac{a_A}{a_B} + \frac{a_B}{a_A} \right). \tag{E.4}$$

The positive frequency Wightman function becomes

$$G^+(\tau_A, \tau'_B) = G^+(\sigma) = -\frac{a_A a_B}{16\pi^2 [\sinh(\frac{a_A(\sigma - i\epsilon - \kappa)}{2}) \sinh(\frac{a_A(\sigma - i\epsilon + \kappa)}{2})]} = [G^+(\tau'_B, \tau_A)]^*, \tag{E.5}$$

Putting (E.2) and (E.5) in (17), we obtain

$$\mathcal{P}_{AB}(\pm\omega, \mp\omega) = -\frac{a_A a_B \alpha_a \mathcal{T}_A^4}{32\pi^2} \int_{-\infty}^{\infty} \frac{d\sigma e^{\pm \frac{i\omega}{2}(1+\alpha_a)\sigma}}{\sinh(\frac{a_A(\sigma+i\epsilon-\kappa)}{2}) \sinh(\frac{a_A(\sigma+i\epsilon+\kappa)}{2})} \int_{-\infty}^{\infty} \frac{dT e^{\pm \frac{i\omega}{2}(1-\alpha_a)T}}{(T^2 - T_1^2)(T^2 - T_2^2)}. \tag{E.6}$$

We are interested to evaluate the quantities $\mathcal{P}_{AB}(\pm\omega)$ when $a_A \neq a_B$. For both the cases $\alpha_a > 1$ and $\alpha_a < 1$, we need to evaluate the T -integrals separately due to their pole structures in the complex T -plane.

For $\alpha_a < 1$:

$\mathcal{P}_{AB}(\omega, -\omega)$: The complex T -integration for $\mathcal{P}_{AB}(\omega, -\omega)$ has the contributing poles at $T_1 = \sigma + i\mathcal{T}_A$ and $T_2 = -\sigma + i\mathcal{T}_A$ in the upper half plane (see fig:(11)). The integration yields

$$\frac{\pi e^{-\omega \mathcal{T}_A (1-\alpha_a)/2}}{4 \sigma \mathcal{T}_A} \left(\frac{e^{-i(1-\alpha_a)\omega\sigma/2}}{-i\mathcal{T}_A + \sigma} + \frac{e^{i(1-\alpha_a)\omega\sigma/2}}{i\mathcal{T}_A + \sigma} \right). \tag{E.7}$$

Putting this into (E.6), we will get,

$$\begin{aligned}
\mathcal{P}_{AB}(\omega, -\omega) &= -\frac{a_A a_B \alpha_a \mathcal{T}_A^3 e^{-\omega \mathcal{T}_A (1-\alpha_a)/2}}{128\pi} \int_{-\infty}^{\infty} \frac{d\sigma}{(\sigma - i\epsilon) [\sinh(\frac{a_A(\sigma+i\epsilon-\kappa)}{2}) \sinh(\frac{a_A(\sigma+i\epsilon+\kappa)}{2})]} \\
&\quad \times \left(\frac{e^{i\omega\sigma}}{\sigma + i\mathcal{T}_A} + \frac{e^{i\omega\sigma\alpha_a}}{\sigma - i\mathcal{T}_A} \right) \\
&= -\frac{a_A a_B \alpha_a \mathcal{T}_A^3 e^{-\omega \mathcal{T}_A (1-\alpha_a)/2}}{128\pi} [\mathcal{P}_{AB,1}(\omega, -\omega) + \mathcal{P}_{AB,2}(\omega, -\omega)]. \tag{E.8}
\end{aligned}$$

The pole at $\sigma = 0$ on the real axis, will be shifted to upper half of the complex σ -plane. The contributing poles are $+i\epsilon$, $+i\mathcal{T}_A$, $\pm\kappa - i\epsilon + \frac{2\pi i n}{a_A}$ ($n = 1, 2, \dots, \infty$) in the upper half plane (see subfigure (a) in figure (12)). The corresponding residues are

$$(2\pi i) \text{Res}(\mathcal{P}_{AB}^{(I)}(\omega, -\omega)) \Big|_{\sigma=i\epsilon} = 0, \tag{E.9}$$

$$(2\pi i) \text{Res}(\mathcal{P}_{AB,2}^{(I)}(\omega, -\omega)) \Big|_{\sigma=i\mathcal{T}_A} = \frac{2\pi e^{-\omega\alpha_a\mathcal{T}_A}}{\mathcal{T}_A \sinh\left(\frac{a_A(-\kappa+i\mathcal{T}_A)}{2}\right) \sinh\left(\frac{a_A(\kappa+i\mathcal{T}_A)}{2}\right)}, \tag{E.10}$$

$$(2\pi i)\text{Res}(\mathcal{P}_{AB}^{(I)}(\omega, -\omega))\Big|_{\sigma=\kappa-i\epsilon+\frac{i2\pi n}{a_A}} = \frac{2\pi i}{\left(\kappa + \frac{2\pi n i}{a_A}\right)\frac{a_A}{2} \sinh(a_A \kappa)} \left[\frac{e^{i\omega[\kappa+\frac{2\pi n i}{a_A}]}}{\kappa + \frac{2\pi i n}{a_A} + i\mathcal{T}_A} + \frac{e^{i\alpha_A \omega[\kappa+\frac{2\pi n i}{a_A}]}}{\kappa + \frac{2\pi i n}{a_A} - i\mathcal{T}_A} \right] \quad (\text{E.11})$$

and

$$(2\pi i)\text{Res}(\mathcal{P}_{AB}^{(I)}(\omega, -\omega))\Big|_{\sigma=-\kappa-i\epsilon+\frac{i2\pi n}{a_A}} = \frac{-2\pi i}{\left(-\kappa + \frac{2\pi n i}{a_A}\right)\frac{a_A}{2} \sinh(a_A \kappa)} \left[\frac{e^{i\omega[-\kappa+\frac{2\pi n i}{a_A}]}}{-\kappa + \frac{2\pi i n}{a_A} + i\mathcal{T}_A} + \frac{e^{i\alpha_A \omega[-\kappa+\frac{2\pi n i}{a_A}]}}{-\kappa + \frac{2\pi i n}{a_A} - i\mathcal{T}_A} \right], \quad (\text{E.12})$$

where we have used, $\cosh(in\pi) = (-1)^n$ and $\sinh(\pm a_A \kappa + in\pi) = \pm \sinh(a_A \kappa)(-1)^n$.

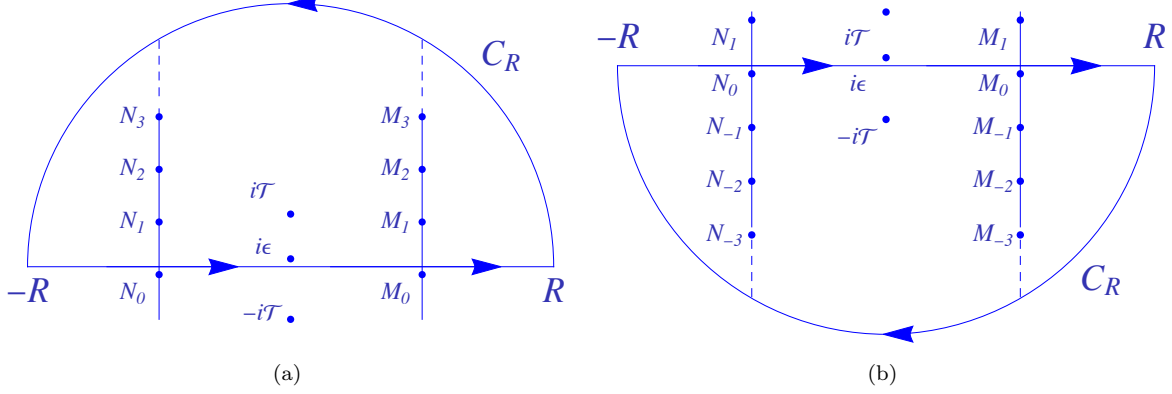


Figure 12: Plots showing contours of integral (a) $\mathcal{P}_{AB}(\omega, -\omega)$, (b) $\mathcal{P}_{AB}(-\omega, \omega)$, where contributing poles are in upper and lower half of the complex- σ plane, respectively. The poles M_n and N_n are defined as $\kappa - i\epsilon + \frac{i2\pi n}{a_A}$ and $-\kappa - i\epsilon + \frac{i2\pi n}{a_A}$, respectively.

$\mathcal{P}_{AB}(-\omega, \omega)$: From (E.6), we have

$$\mathcal{P}_{AB}(-\omega, \omega) = -\frac{a_A a_B \alpha_a \mathcal{T}_A^4}{32\pi^2} \int_{-\infty}^{\infty} \frac{d\sigma e^{-i\frac{\omega\sigma}{2}(1+\alpha_a)}}{\sinh\left(\frac{a_A(\sigma+i\epsilon-\kappa)}{2}\right) \sinh\left(\frac{a_A(\sigma+i\epsilon+\kappa)}{2}\right)} \int_{-\infty}^{\infty} \frac{dT e^{-i\frac{\omega T}{2}(1-\alpha_a)}}{(T^2 - T_1^2)(T^2 - T_2^2)}. \quad (\text{E.13})$$

The complex T -integration has the contributing poles at $T = -T_1 = -\sigma - i\mathcal{T}_A$ and $T = -T_2 = \sigma - i\mathcal{T}_A$ in the lower half plane (see fig:(11)). The integration yields

$$\frac{\pi e^{-\omega\mathcal{T}_A(1-\alpha_a)/2}}{4\sigma\mathcal{T}_A} \left(\frac{e^{-i\frac{\omega\sigma}{2}(1-\alpha_a)}}{\sigma - i\mathcal{T}_A} + \frac{e^{i\frac{\omega\sigma}{2}(1-\alpha_a)}}{\sigma + i\mathcal{T}_A} \right). \quad (\text{E.14})$$

Putting this into (E.13), we obtain

$$\begin{aligned} \mathcal{P}_{AB}(-\omega, \omega) &= -\frac{a_A a_B \alpha_a \mathcal{T}_A^3 e^{-\omega\mathcal{T}_A(1-\alpha_a)/2}}{128\pi} \int_{-\infty}^{\infty} \frac{d\sigma}{(\sigma - i\epsilon) [\sinh\left(\frac{a_A(\sigma+i\epsilon-\kappa)}{2}\right) \sinh\left(\frac{a_A(\sigma+i\epsilon+\kappa)}{2}\right)]} \\ &\quad \times \left(\frac{e^{-i\omega\sigma}}{\sigma - i\mathcal{T}_A} + \frac{e^{-i\omega\sigma\alpha_a}}{\sigma + i\mathcal{T}_A} \right) \\ &= -\frac{a_A a_B \alpha_a \mathcal{T}_A^3 e^{-\omega\mathcal{T}_A(1-\alpha_a)/2}}{128\pi} [\mathcal{P}_{AB,1}(-\omega, \omega) + \mathcal{P}_{AB,2}(-\omega, \omega)]. \end{aligned} \quad (\text{E.15})$$

The contributing poles are $-i\mathcal{T}_A$, $\pm \kappa + i\epsilon - \frac{2\pi i n}{a_A}$ ($n = 0, 1, \dots, \infty$) in the lower half plane (see subfigure (b) in figure (12)). The corresponding residues are

$$(-2\pi i)\text{Res}(\mathcal{P}_{AB,2}^{(I)}(-\omega, \omega))\Big|_{\sigma=-i\mathcal{T}_A} = \frac{2\pi e^{-\omega\alpha_a \mathcal{T}_A}}{\mathcal{T}_A \sinh\left(\frac{a_A(\kappa-i\mathcal{T}_A)}{2}\right) \sinh\left(\frac{a_A(-\kappa-i\mathcal{T}_A)}{2}\right)}, \quad (\text{E.16})$$

$$(-2\pi i)\text{Res}(\mathcal{P}_{AB}^{(I)}(-\omega, \omega))\Big|_{\sigma=\kappa-i\epsilon-\frac{i2\pi n}{a_A}} = \frac{-2\pi i}{\left(\kappa - \frac{2\pi i n}{a_A}\right)\frac{a_A}{2} \sinh(a_A \kappa)} \left[\frac{e^{-i\omega[k-\frac{2\pi i n}{a_A}]}}{k - \frac{2\pi i n}{a_A} - i\mathcal{T}_A} + \frac{e^{-i\omega\alpha_a[k-\frac{2\pi i n}{a_A}]}}{k - \frac{2\pi i n}{a_A} + i\mathcal{T}_A} \right], \quad (\text{E.17})$$

and

$$(-2\pi i)\text{Res}(\mathcal{P}_{AB}^{(I)}(-\omega, \omega))\Big|_{\sigma=-\kappa-i\epsilon-\frac{i2\pi n}{a_A}} = \frac{-2\pi i}{\left(k + \frac{2\pi in}{a_A}\right)\frac{a_A}{2}\sinh(a_A\kappa)} \left[\frac{e^{i\omega[k+\frac{2\pi in}{a_A}]}}{-k - \frac{2\pi in}{a_A} - iT_A} + \frac{e^{i\omega\alpha_a[k+\frac{2\pi in}{a_A}]}}{-k - \frac{2\pi in}{a_A} + iT_A} \right], \quad (\text{E.18})$$

where we have used, $\cosh(-in\pi) = (-1)^n$ and $\sinh(\pm a_A\kappa - in\pi) = \pm \sinh(a_A\kappa)(-1)^n$.

In $\mathcal{P}_{AB}(\omega, -\omega) - \mathcal{P}_{AB}(-\omega, \omega)$, residue given in (E.10) will cancel out with residue (E.16), and for all $n > 0$ residues given in (E.11) and (E.12) cancel out with residues in (E.18) and (E.17), respectively. The difference, $\mathcal{P}_{AB}(\omega, -\omega) - \mathcal{P}_{AB}(-\omega, \omega)$ can be obtained by adding (E.17) and (E.18) for $n = 0$ (multiplied with the factor $\frac{-a_A a_B \alpha_a \mathcal{T}_A^3 e^{-\omega \mathcal{T}_A (1-\alpha_a)/2}}{128\pi}$), given in (27).

For $\alpha_a > 1$:

$\mathcal{P}_{AB}(\omega, -\omega)$: From (E.6), we have

$$\mathcal{P}_{AB}(\omega, -\omega) = -\frac{a_A a_B \alpha_a \mathcal{T}_A^4}{32\pi^2} \int_{-\infty}^{\infty} \frac{d\sigma e^{\frac{i\omega\sigma}{2}(1+\alpha_a)}}{\sinh\left(\frac{a_A(\sigma+i\epsilon-\kappa)}{2}\right)\sinh\left(\frac{a_A(\sigma+i\epsilon+\kappa)}{2}\right)} \int_{-\infty}^{\infty} \frac{dT e^{-\frac{i\omega T}{2}(\alpha_a-1)}}{(T^2 - T_1^2)(T^2 - T_2^2)}. \quad (\text{E.19})$$

The complex T -integration has the contributing poles at $T = -T_1 = -\sigma - iT_A$ and $T = -T_2 = \sigma - iT_A$ in the lower half plane (see fig:(11)). The integration yields

$$\frac{\pi e^{-\omega \mathcal{T}_A (\alpha_a - 1)/2}}{4\sigma \mathcal{T}_A} \left(\frac{e^{-\frac{i\omega\sigma}{2}(\alpha_a-1)}}{\sigma - iT_A} + \frac{e^{\frac{i\omega\sigma}{2}(\alpha_a-1)}}{\sigma + iT_A} \right). \quad (\text{E.20})$$

Putting this into (E.19), we will get,

$$\begin{aligned} \mathcal{P}_{AB}(\omega, -\omega) &= -\frac{a_A a_B \alpha_a \mathcal{T}_A^3 e^{-\omega \mathcal{T}_A (\alpha_a - 1)/2}}{128\pi} \int_{-\infty}^{\infty} \frac{d\sigma}{(\sigma - i\epsilon) [\sinh\left(\frac{a_A(\sigma+i\epsilon-\kappa)}{2}\right)\sinh\left(\frac{a_A(\sigma+i\epsilon+\kappa)}{2}\right)]} \\ &\quad \times \left(\frac{e^{i\omega\sigma}}{\sigma - iT_A} + \frac{e^{i\omega\sigma\alpha_a}}{\sigma + iT_A} \right) \\ &= -\frac{a_A a_B \alpha_a \mathcal{T}_A^3 e^{-\omega \mathcal{T}_A (\alpha_a - 1)/2}}{128\pi} [\mathcal{P}_{AB,1}(\omega, -\omega) + \mathcal{P}_{AB,2}(\omega, -\omega)]. \end{aligned} \quad (\text{E.21})$$

The contributing poles are $i\epsilon$, $i\mathcal{T}_A$, $\pm\kappa - i\epsilon + \frac{2\pi in}{a_A}$ ($n = 1, 2, \dots, \infty$) in the upper half plane (see subfigure (a) in figure (12)). The corresponding residues are

$$(2\pi i)\text{Res}(\mathcal{P}_{AB}^{(I)}(\omega, -\omega))\Big|_{\sigma=i\epsilon} = 0, \quad (\text{E.22})$$

$$(2\pi i)\text{Res}(\mathcal{P}_{AB,1}^{(I)}(\omega, -\omega))\Big|_{\sigma=i\mathcal{T}_A} = \frac{2\pi e^{-\omega \mathcal{T}_A}}{\mathcal{T}_A \sinh\left(\frac{a_A(-\kappa+i\mathcal{T}_A)}{2}\right)\sinh\left(\frac{a_A(\kappa+i\mathcal{T}_A)}{2}\right)}, \quad (\text{E.23})$$

$$(2\pi i)\text{Res}(\mathcal{P}_{AB}^{(I)}(\omega, -\omega))\Big|_{\sigma=\kappa-i\epsilon+\frac{i2\pi n}{a_A}} = \frac{2\pi i}{\left(\kappa + \frac{2\pi in}{a_A}\right)\frac{a_A}{2}\sinh(a_A\kappa)} \left[\frac{e^{i\omega[\kappa+\frac{2\pi in}{a_A}]}}{\kappa + \frac{2\pi in}{a_A} - iT_A} + \frac{e^{i\alpha_a\omega[\kappa+\frac{2\pi in}{a_A}]}}{\kappa + \frac{2\pi in}{a_A} + iT_A} \right], \quad (\text{E.24})$$

and

$$(2\pi i)\text{Res}(\mathcal{P}_{AB}^{(I)}(\omega, -\omega))\Big|_{\sigma=-\kappa-i\epsilon+\frac{i2\pi n}{a_A}} = \frac{-2\pi i}{\left(-\kappa + \frac{2\pi in}{a_A}\right)\frac{a_A}{2}\sinh(a_A\kappa)} \left[\frac{e^{i\omega[-\kappa+\frac{2\pi in}{a_A}]}}{-\kappa + \frac{2\pi in}{a_A} - iT_A} + \frac{e^{i\alpha_a\omega[-\kappa+\frac{2\pi in}{a_A}]}}{-\kappa + \frac{2\pi in}{a_A} + iT_A} \right], \quad (\text{E.25})$$

where we have used, $\cosh(in\pi) = (-1)^n$ and $\sinh(\pm a_A\kappa + in\pi) = \pm \sinh(a_A\kappa)(-1)^n$.

$\mathcal{P}_{AB}(-\omega, \omega)$: From (E.6), we have

$$\mathcal{P}_{AB}(-\omega, \omega) = -\frac{a_A a_B \alpha_a \mathcal{T}_A^4}{32\pi^2} \int_{-\infty}^{\infty} \frac{d\sigma e^{-\frac{i\omega\sigma}{2}(1+\alpha_a)}}{\sinh\left(\frac{a_A(\sigma+i\epsilon-\kappa)}{2}\right) \sinh\left(\frac{a_A(\sigma+i\epsilon+\kappa)}{2}\right)} \int_{-\infty}^{\infty} \frac{dT e^{\frac{i\omega T}{2}(\alpha_a-1)}}{(T^2 - T_1^2)(T^2 - T_2^2)}. \quad (\text{E.26})$$

The complex T -integration has the contributing poles at $T = T_1 = \sigma + i\mathcal{T}_A$ and $T = T_2 = -\sigma + i\mathcal{T}_A$ in the upper half plane (see fig:(11)). The integration yields

$$\frac{\pi e^{-\omega\mathcal{T}_A(\alpha_a-1)/2}}{4\sigma\mathcal{T}_A} \left(\frac{e^{-i(\alpha_a-1)\omega\sigma/2}}{\sigma - i\mathcal{T}_A} + \frac{e^{i(\alpha_a-1)\omega\sigma/2}}{\sigma + i\mathcal{T}_A} \right). \quad (\text{E.27})$$

Putting this into (E.26), we obtain

$$\begin{aligned} \mathcal{P}_{AB}(-\omega, \omega) &= -\frac{a_A a_B \alpha_a \mathcal{T}_A^3 e^{-\omega\mathcal{T}_A(\alpha_a-1)/2}}{128\pi} \int_{-\infty}^{\infty} \frac{d\sigma}{(\sigma - i\epsilon) [\sinh\left(\frac{a_A(\sigma+i\epsilon-\kappa)}{2}\right) \sinh\left(\frac{a_A(\sigma+i\epsilon+\kappa)}{2}\right)]} \\ &\quad \times \left(\frac{e^{-i\omega\sigma}}{\sigma + i\mathcal{T}_A} + \frac{e^{-i\omega\sigma\alpha_a}}{\sigma - i\mathcal{T}_A} \right) \\ &= -\frac{a_A a_B \alpha_a \mathcal{T}_A^3 e^{-\omega\mathcal{T}_A(\alpha_a-1)/2}}{128\pi} [\mathcal{P}_{AB,1}(-\omega, \omega) + \mathcal{P}_{AB,2}(-\omega, \omega)]. \end{aligned} \quad (\text{E.28})$$

The contributing poles are $-i\mathcal{T}_A$, $\pm\kappa - i\epsilon - \frac{2\pi in}{a_A}$ ($n = 0, 1, \dots, \infty$) in the lower half plane (see subfigure (b) in figure (12)). The corresponding residues are

$$(-2\pi i) \text{Res}(\mathcal{P}_{AB,1}^{(I)}(-\omega, \omega)) \Big|_{\sigma=-i\mathcal{T}_A} = \frac{2\pi e^{-\omega\mathcal{T}_A}}{\mathcal{T}_A \sinh\left(\frac{a_A(\kappa-i\mathcal{T}_A)}{2}\right) \sinh\left(\frac{a_A(-\kappa-i\mathcal{T}_A)}{2}\right)}, \quad (\text{E.29})$$

$$(-2\pi i) \text{Res}(\mathcal{P}_{AB}^{(I)}(-\omega, \omega)) \Big|_{\sigma=\kappa-i\epsilon-\frac{i2\pi n}{a_A}} = \frac{-2\pi i}{\left(k - \frac{2\pi in}{a_A}\right) \frac{a_A}{2} \sinh(a_A \kappa)} \left[\frac{e^{-i\omega[k-\frac{2\pi in}{a_A}]}}{k - \frac{2\pi in}{a_A} + i\mathcal{T}_A} + \frac{e^{-i\omega\alpha_a[k-\frac{2\pi in}{a_A}]}}{k - \frac{2\pi in}{a_A} - i\mathcal{T}_A} \right], \quad (\text{E.30})$$

and

$$(-2\pi i) \text{Res}(\mathcal{P}_{AB}^{(I)}(-\omega, \omega)) \Big|_{\sigma=-\kappa-i\epsilon-\frac{i2\pi n}{a_A}} = \frac{2\pi i}{\left(-k - \frac{2\pi in}{a_A}\right) \frac{a_A}{2} \sinh(a_A \kappa)} \left[\frac{e^{i\omega[k+\frac{2\pi in}{a_A}]}}{-k - \frac{2\pi in}{a_A} + i\mathcal{T}_A} + \frac{e^{i\omega\alpha_a[k+\frac{2\pi in}{a_A}]}}{-k - \frac{2\pi in}{a_A} - i\mathcal{T}_A} \right], \quad (\text{E.31})$$

where we have used, $\cosh(-in\pi) = (-1)^n$ and $\sinh(\pm a_A \kappa - in\pi) = \pm \sinh(a_A \kappa) (-1)^n$.

In $\mathcal{P}_{AB}(\omega, -\omega) - \mathcal{P}_{AB}(-\omega, \omega)$, residue given in (E.23) cancel out with residue in (E.29) and for all $n > 0$ residues given in (E.24) and (E.25) cancel out with residues in (E.31) and (E.30), respectively. The difference, $\mathcal{P}_{AB}(\omega, -\omega) - \mathcal{P}_{AB}(-\omega, \omega)$ can be obtained by adding (E.31) and (E.30) for $n = 0$ (multiplied with the factor $\frac{-a_A a_B \alpha_a \mathcal{T}_A^3 e^{-\omega\mathcal{T}_A(1-\alpha_a)/2}}{128\pi}$), given in (28).

E.2 Acceleration in Opposite Direction

If the detector A and B are accelerating anti-parallelly, their trajectories are given by (A.3). Therefore, denominator of the green function can be calculated as

$$\begin{aligned} &(t_A - t'_B - i\epsilon)^2 - |\bar{x}_A - \bar{x}'_B|^2 \\ &= \left(\frac{1}{a_A} \sinh(a_A \tau_A) - \frac{1}{a_B} \sinh(a_B \tau'_B) - i\epsilon \right)^2 - \left(\frac{1}{a_A} \cosh(a_A \tau_A) + \frac{1}{a_B} \cosh(a_B \tau'_B) \right)^2 \\ &= -\frac{1}{a_A^2} - \frac{1}{a_B^2} - \frac{2}{a_A a_B} (\cosh(a_A \tau_A) + \cosh(a_B \tau'_B)) + i\epsilon \\ &= -\frac{2}{a_A a_B} (\cosh(a_A \sigma + i\epsilon) + \cosh(a_A \kappa)) \\ &= -\frac{4}{a_A a_B} \cosh\left(\frac{a_A(\sigma + i\epsilon + \kappa)}{2}\right) \cosh\left(\frac{a_A(\sigma + i\epsilon - \kappa)}{2}\right), \end{aligned} \quad (\text{E.32})$$

where in the third equality, we have used (A.4), (D.2) and (E.4). The corresponding Wightman function is

$$G^+(\tau_A, \tau'_B) = G^+(\sigma) = + \frac{a_A a_B}{16\pi^2 [\cosh(\frac{a_A(\sigma+i\epsilon-\kappa)}{2}) \cosh(\frac{a_A(\sigma+i\epsilon+\kappa)}{2})]} = [G^+(\tau'_B, \tau_A)]^* . \quad (\text{E.33})$$

The Wightman function has poles at

$$\sigma = \pm\kappa - i\epsilon \pm i \frac{\pi(2n+1)}{a_A}; \quad n = 0, 1, 2, \dots \infty \quad (\text{E.34})$$

As there is no poles on the real axis, the absence or presence of the ‘ $i\epsilon$ ’ in the green function, will not effect the complex integral of σ . We will drop the ‘ $i\epsilon$ ’ from the Wightman function. We also can check that

$$\omega(\tau_A - \tau_B) = \omega(\tau_A + \alpha_a \tau'_A) = \frac{\omega\sigma}{2}(1 - \alpha_a) + \frac{\omega T}{2}(1 + \alpha_a) . \quad (\text{E.35})$$

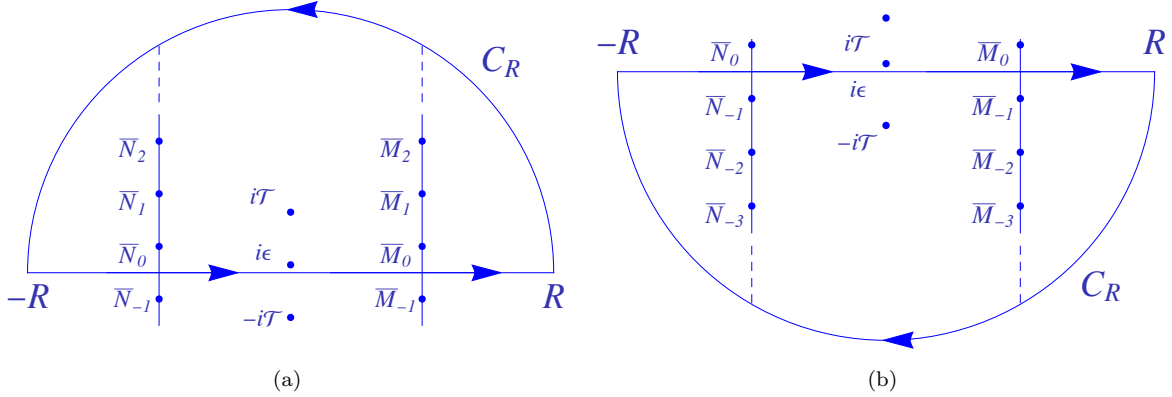


Figure 13: Plots showing contours of integral (a) $\mathcal{P}_{AB}(\omega, -\omega)$, (b) $\mathcal{P}_{AB}(-\omega, \omega)$, where contributing poles are in upper and lower half of the complex- σ plane, respectively. The poles \bar{M}_n and \bar{N}_n are defined as $\kappa + \frac{i\pi(2n+1)}{a_A}$ and $-\kappa + \frac{i\pi(2n+1)}{a_A}$, respectively.

Using (E.33), (E.35) and (E.1) in (17), we obtain expression of \mathcal{P}_{AB} , as

$$\mathcal{P}_{AB}(\pm\omega, \mp\omega) = - \frac{a_A a_B \alpha_a \mathcal{T}_A^4}{32\pi^2} \int_{-\infty}^{\infty} \frac{d\sigma e^{\pm \frac{i\omega}{2}(1-\alpha_a)\sigma}}{\cosh(\frac{a_A(\sigma-\kappa)}{2}) \cosh(\frac{a_A(\sigma+\kappa)}{2})} \int_{-\infty}^{\infty} \frac{dT e^{\pm \frac{i\omega}{2}(1+\alpha_a)T}}{(T^2 - T_1^2)(T^2 - T_2^2)} . \quad (\text{E.36})$$

$\mathcal{P}_{AB}(\omega, -\omega)$: From (E.36), the complex T -integration has the contributing poles at $T = T_1 = \sigma + i\mathcal{T}_A$ and $T = T_2 = -\sigma + i\mathcal{T}_A$ in the upper half plane (see fig:(11)). The integration yields

$$\frac{\pi e^{-\frac{1}{2}\omega\mathcal{T}_A(\alpha_a+1)}}{4\sigma\mathcal{T}_A} \left(\frac{e^{\frac{i}{2}(\alpha_a+1)\omega\sigma}}{\sigma + i\mathcal{T}_A} + \frac{e^{-\frac{i}{2}(\alpha_a+1)\omega\sigma}}{\sigma - i\mathcal{T}_A} \right) . \quad (\text{E.37})$$

Putting this into (E.36)

$$\begin{aligned} \mathcal{P}_{AB}(\omega, -\omega) &= - \frac{a_A a_B \alpha_a \mathcal{T}_A^3 e^{-(1+\alpha_a)\mathcal{T}_A\omega/2}}{128\pi} \\ &\times \int_{-\infty}^{\infty} \frac{d\sigma}{(\sigma - i\epsilon) [\cosh(\frac{a_A(\sigma-\kappa)}{2}) \cosh(\frac{a_A(\sigma+\kappa)}{2})]} \left(\frac{e^{i\omega\sigma}}{\sigma + i\mathcal{T}_A} + \frac{e^{-i\alpha_a\omega\sigma}}{\sigma - i\mathcal{T}_A} \right) \\ &= - \frac{a_A a_B \alpha_a \mathcal{T}_A^3 e^{-(1+\alpha_a)\mathcal{T}_A\omega/2}}{128\pi} [\mathcal{P}_{AB,1}(\omega, -\omega) + \mathcal{P}_{AB,2}(\omega, -\omega)] . \end{aligned} \quad (\text{E.38})$$

The contributing poles are $+i\epsilon, \pm\kappa \pm \frac{i\pi(2n+1)}{a_A}$ ($n = 0, 1, \dots, \infty$) for the upper and lower half planes. The residues of the first term in the upper half plane (see subfigure (a) of figure (13)) are obtained as

$$\text{Res}(\mathcal{P}_{AB,1}^{(J)}(\omega, -\omega)) \Big|_{\sigma=i\epsilon} = \frac{2\pi}{\mathcal{T}_A \cosh^2(\frac{a_A\kappa}{2})} \quad (\text{E.39})$$

and

$$\begin{aligned}
& (2\pi i)\text{Res}(\mathcal{P}_{AB,1}^{(I)}(\omega, -\omega))\Big|_{\sigma=\kappa+\frac{\pi i(2n+1)}{a_A}} + (2\pi i)\text{Res}(\mathcal{P}_{AB,1}^{(I)}(\omega, -\omega))\Big|_{\sigma=-\kappa+\frac{\pi i(2n+1)}{a_A}} \\
&= \frac{4\pi i \operatorname{csch}(a_A \kappa)}{a_A \sinh^2\left(\frac{(2n+1)i\pi}{2}\right)} \left(\frac{e^{i\omega\left[k+\frac{(2n+1)i\pi}{a_A}\right]}}{\left(k+\frac{(2n+1)i\pi}{a_A}\right)\left(k+\frac{(2n+1)i\pi}{a_A}+i\mathcal{T}_A\right)} - \frac{e^{i\omega\left[-k+\frac{(2n+1)i\pi}{a_A}\right]}}{\left(k-\frac{(2n+1)i\pi}{a_A}\right)\left(k-\frac{(2n+1)i\pi}{a_A}-i\mathcal{T}_A\right)} \right), \tag{E.40}
\end{aligned}$$

where we have used $\cosh(\pm ak \pm (2n+1)\frac{i\pi}{2}) = \sinh(\pm ak) \sinh(\pm(2n+1)\frac{i\pi}{2})$ and for the second term in the lower half plane (see subfigure (b) of figure (13)), we obtain

$$\begin{aligned}
& (-2\pi i)\text{Res}(\mathcal{P}_{AB,2}^{(I)}(\omega, -\omega))\Big|_{\sigma=\kappa-\frac{\pi i(2n+1)}{a_A}} + (-2\pi i)\text{Res}(\mathcal{P}_{AB,2}^{(I)}(\omega, -\omega))\Big|_{\sigma=-\kappa-\frac{\pi i(2n+1)}{a_A}} \\
&= \frac{-4\pi i \operatorname{csch}(a_A \kappa)}{a_A \sinh^2\left(-\frac{(2n+1)i\pi}{2}\right)} \left(\frac{e^{-i\omega\alpha_a\left[k-\frac{(2n+1)i\pi}{a_A}\right]}}{\left(k-\frac{(2n+1)i\pi}{a_A}\right)\left(k-\frac{(2n+1)i\pi}{a_A}-i\mathcal{T}_A\right)} - \frac{e^{-i\omega\alpha_a\left[-k-\frac{(2n+1)i\pi}{a_A}\right]}}{\left(k+\frac{(2n+1)i\pi}{a_A}\right)\left(k+\frac{(2n+1)i\pi}{a_A}+i\mathcal{T}_A\right)} \right). \tag{E.41}
\end{aligned}$$

$\mathcal{P}_{AB}(-\omega, \omega)$: From (E.36), the complex T -integration has the contributing poles at $T = -T_1 = -\sigma - i\mathcal{T}_A$ and $\bar{T} = -T_2 = \sigma - i\mathcal{T}_A$ in the lower half plane (see fig:(11)). The integration yields

$$\frac{\pi e^{-\frac{1}{2}(\alpha_a+1)\mathcal{T}_A\omega}}{4\sigma\mathcal{T}_A} \left(\frac{e^{\frac{i}{2}(\alpha_a+1)\sigma\omega}}{\sigma+i\mathcal{T}_A} + \frac{e^{-\frac{i}{2}(\alpha_a+1)\sigma\omega}}{\sigma-i\mathcal{T}_A} \right). \tag{E.42}$$

Putting this into (E.36), we obtain

$$\begin{aligned}
\mathcal{P}_{AB}(-\omega, \omega) &= -\frac{a_A a_B \alpha_a \mathcal{T}_A^3 e^{-(1+\alpha_a)\mathcal{T}_A\omega/2}}{128\pi} \\
&\times \int_{-\infty}^{\infty} \frac{d\sigma}{(\sigma-i\epsilon)[\cosh\left(\frac{a_A(\sigma-\kappa)}{2}\right)\cosh\left(\frac{a_A(\sigma+\kappa)}{2}\right)]} \left(\frac{e^{i\alpha_a\omega\sigma}}{\sigma+i\mathcal{T}_A} + \frac{e^{-i\omega\sigma}}{\sigma-i\mathcal{T}_A} \right) \\
&= -\frac{a_A a_B \alpha_a \mathcal{T}_A^3 e^{-(1+\alpha_a)\mathcal{T}_A\omega/2}}{128\pi} [\mathcal{P}_{AB,1}(-\omega, \omega) + \mathcal{P}_{AB,2}(-\omega, \omega)]. \tag{E.43}
\end{aligned}$$

The contributing poles are $+i\epsilon, \pm\kappa \pm \frac{i\pi(2n+1)}{a_A}$ ($n = 0, 1, \dots, \infty$) for the upper half plane and lower half plane. The corresponding residues for the first term in the upper half plane (see subfigure (a) of figure (13)), are

$$\text{Res}(\mathcal{P}_{AB,1}^{(I)}(-\omega, \omega))\Big|_{\sigma=i\epsilon} = \frac{2\pi}{\mathcal{T}_A \cosh^2\left(\frac{a_A\kappa}{2}\right)} \tag{E.44}$$

and

$$\begin{aligned}
& (2\pi i)\text{Res}(\mathcal{P}_{AB,1}^{(I)}(-\omega, \omega))\Big|_{\sigma=\kappa+\frac{\pi i(2n+1)}{a_A}} + (2\pi i)\text{Res}(\mathcal{P}_{AB,1}^{(I)}(-\omega, \omega))\Big|_{\sigma=-\kappa+\frac{\pi i(2n+1)}{a_A}} \\
&= \frac{4\pi i \operatorname{csch}(a_A \kappa)}{a_A \sinh^2\left(\frac{(2n+1)i\pi}{2}\right)} \left(\frac{e^{i\omega\alpha_a\left[k+\frac{(2n+1)i\pi}{a_A}\right]}}{\left(k+\frac{(2n+1)i\pi}{a_A}\right)\left(k+\frac{(2n+1)i\pi}{a_A}+i\mathcal{T}_A\right)} - \frac{e^{i\omega\alpha_a\left[-k+\frac{(2n+1)i\pi}{a_A}\right]}}{\left(k-\frac{(2n+1)i\pi}{a_A}\right)\left(k-\frac{(2n+1)i\pi}{a_A}-i\mathcal{T}_A\right)} \right). \tag{E.45}
\end{aligned}$$

For the second term in the lower half plane (see subfigure (b) of figure (13)), we obtain

$$\begin{aligned}
& (-2\pi i)\text{Res}(\mathcal{P}_{AB,2}^{(I)}(-\omega, \omega))\Big|_{\sigma=\kappa-\frac{\pi i(2n+1)}{a_A}} + (-2\pi i)\text{Res}(\mathcal{P}_{AB,2}^{(I)}(-\omega, \omega))\Big|_{\sigma=-\kappa-\frac{\pi i(2n+1)}{a_A}} \\
&= \frac{-4\pi i \operatorname{csch}(a_A \kappa)}{a_A \sinh^2\left(-\frac{(2n+1)i\pi}{2}\right)} \left(\frac{e^{-i\omega\left[k-\frac{(2n+1)i\pi}{a_A}\right]}}{\left(k-\frac{(2n+1)i\pi}{a_A}\right)\left(k-\frac{(2n+1)i\pi}{a_A}-i\mathcal{T}_A\right)} - \frac{e^{-i\omega\left[-k-\frac{(2n+1)i\pi}{a_A}\right]}}{\left(k+\frac{(2n+1)i\pi}{a_A}\right)\left(k+\frac{(2n+1)i\pi}{a_A}+i\mathcal{T}_A\right)} \right). \tag{E.46}
\end{aligned}$$

So, in $\Delta\mathcal{P}_{AB}$, residues in (E.39), (E.40), and (E.41) cancel out with residues in (E.44), (E.46) and (E.45), respectively. Hence, $\Delta\mathcal{P}_{AB}$ vanishes for anti-parallel acceleration of the detectors.

References

- [1] J. Gemmer, M. Michel, and G. Mahler, *Quantum Thermodynamics*, vol. 657 of *Lecture Notes in Physics*. Springer-Verlag, Berlin Heidelberg, Germany, 2004.
- [2] C. M. Bender, D. C. Brody, and B. K. Meister, “Quantum mechanical carnot engine,” *Journal of Physics A: Mathematical and General*, vol. 33, pp. 4427–4436, jun 2000.
- [3] T. D. Kieu, “The second law, maxwell’s demon, and work derivable from quantum heat engines,” *Phys. Rev. Lett.*, vol. 93, p. 140403, Sep 2004.
- [4] T. D. Kieu, “Quantum heat engines, the second law and maxwell’s daemon,” *The European Physical Journal D - Atomic, Molecular, Optical and Plasma Physics*, vol. 39, no. 1, pp. 115–128, 2006.
- [5] H. T. Quan, Y.-x. Liu, C. P. Sun, and F. Nori, “Quantum thermodynamic cycles and quantum heat engines,” *Physical Review E*, vol. 76, Sep 2007.
- [6] S. Çakmak, M. Çandır, and F. Altintas, “Construction of a quantum carnot heat engine cycle,” *Quantum Information Processing*, vol. 19, no. 9, p. 314, 2020.
- [7] S. W. HAWKING, “Black hole explosions?,” *Nature*, vol. 248, no. 5443, pp. 30–31, 1974.
- [8] S. W. Hawking, “Particle creation by black holes,” *Comm. Math. Phys.*, vol. 43, no. 3, pp. 199–220, 1975.
- [9] P. C. W. Davies, “Scalar particle production in Schwarzschild and Rindler metrics,” *J. Phys.*, vol. A8, pp. 609–616, 1975.
- [10] W. Unruh, “Notes on black hole evaporation,” *Phys.Rev.*, vol. D14, p. 870, 1976.
- [11] W. G. Unruh and R. M. Wald, “What happens when an accelerating observer detects a rindler particle,” *Phys. Rev. D*, vol. 29, pp. 1047–1056, Mar 1984.
- [12] E. Arias, T. R. de Oliveira, and M. S. Sarandy, “The unruh quantum otto engine,” *Journal of High Energy Physics*, vol. 2018, no. 2, p. 168, 2018.
- [13] F. Gray and R. B. Mann, “Scalar and fermionic unruh otto engines,” *Journal of High Energy Physics*, vol. 2018, no. 11, p. 174, 2018.
- [14] H. Xu and M.-H. Yung, “Unruh quantum otto heat engine with level degeneracy,” *Physics Letters B*, vol. 801, p. 135201, 2020.
- [15] G. R. Kane and B. R. Majhi, “Entangled quantum unruh otto engine is more efficient,” *Phys. Rev. D*, vol. 104, p. L041701, Aug 2021.
- [16] E. Arias, J. G. Dueñas, G. Menezes, and N. F. Svaiter, “Boundary effects on radiative processes of two entangled atoms,” *Journal of High Energy Physics*, vol. 2016, no. 7, p. 147, 2016.
- [17] C. Rodríguez-Camargo, G. Menezes, and N. Svaiter, “Finite-time response function of uniformly accelerated entangled atoms,” *Annals of Physics*, vol. 396, pp. 266–291, 2018.
- [18] G. Picanço, N. F. Svaiter, and C. A. D. Zarro, “Radiative processes of entangled detectors in rotating frames,” *Journal of High Energy Physics*, vol. 2020, no. 8, p. 25, 2020.
- [19] S. Barman and B. R. Majhi, “Radiative process of two entangled uniformly accelerated atoms in a thermal bath: a possible case of anti-unruh event,” *Journal of High Energy Physics*, vol. 2021, no. 3, p. 245, 2021.
- [20] P. M. Alsing, D. McMahon, and G. J. Milburn, “Teleportation in a non-inertial frame,” *Journal of Optics B: Quantum and Semiclassical Optics*, vol. 6, pp. S834–S843, jul 2004.
- [21] I. Fuentes-Schuller and R. B. Mann, “Alice falls into a black hole: Entanglement in noninertial frames,” *Phys. Rev. Lett.*, vol. 95, p. 120404, Sep 2005.

- [22] T. G. Downes, I. Fuentes, and T. C. Ralph, “Entangling moving cavities in noninertial frames,” *Phys. Rev. Lett.*, vol. 106, p. 210502, May 2011.
- [23] P. Chowdhury and B. R. Majhi, “Fate of entanglement between two Unruh-DeWitt detectors due to their motion and background temperature,” arXiv: 2110.11260.
- [24] J.-i. Koga, K. Maeda, and G. Kimura, “Entanglement extracted from vacuum into accelerated Unruh-DeWitt detectors and energy conservation,” *Phys. Rev. D*, vol. 100, no. 6, p. 065013, 2019.
- [25] D. Barman, S. Barman, and B. R. Majhi, “Role of thermal field in entanglement harvesting between two accelerated unruh-dewitt detectors,” *Journal of High Energy Physics*, vol. 2021, no. 7, p. 124, 2021.
- [26] N. D. Birrell and P. C. W. Davies, *Quantum fields in curved space*. Cambridge Monographs on Mathematical Physics, Cambridge University Press, 1984.
- [27] R. H. Dicke, “Coherence in spontaneous radiation processes,” *Phys. Rev.*, vol. 93, pp. 99–110, Jan 1954.
- [28] K. K. Ng, R. B. Mann, and E. Martín-Martínez, “New techniques for entanglement harvesting in flat and curved spacetimes,” *Phys. Rev. D*, vol. 97, p. 125011, Jun 2018.
- [29] J.-i. Koga, G. Kimura, and K. Maeda, “Quantum teleportation in vacuum using only unruh-dewitt detectors,” *Phys. Rev. A*, vol. 97, p. 062338, Jun 2018.
- [30] Peskin and Schroeder, *An Introduction to Quantum Field Theory*. Westview Press, 1 ed., 2015.